A geometrically exact micromorphic model for elastic metallic foams accounting for affine microstructure. Modelling, existence of minimizers, identification of moduli and computational results.

Patrizio Neff *
Department of Mathematics
Darmstadt University of Technology, Germany

Samuel Forest
Ecole National Superieure des Mines de Paris
Centre des Materiaux, Evry, France

6th December 2004

Abstract

We investigate a geometrically exact generalized continua of micromorphic type in the sense of Eringen for the phenomenological description of metallic foams. The two-field problem for the macrodeformation φ and the "affine microdeformation" $\overline{P} \in \mathrm{GL}^+(3,\mathbb{R})$ in the quasistatic, conservative elastic case is investigated in a variational form. The elastic stress-strain relation is taken for simplicity as physically linear.

Depending on material constants different mathematical existence theorems in Sobolev-spaces are given for the resulting nonlinear boundary value problems. These results extend existence results obtained by the first author for the micro-incompressible case $\overline{P} \in \mathrm{SL}(3,\mathbb{R})$ and the micropolar case $\overline{P} \in \mathrm{SO}(3,\mathbb{R})$.

In order to mathematically treat external loads for large deformations a new condition, called bounded external work, has to be included, overcoming the conditional coercivity of the formulation. The observed possible lack of coercivity is related to fracture of the substructure of the metallic foam.

We identify the relevant effective material parameters by comparison with the linear micromorphic model and its classical response for large scale samples. We corroborate the performance of the micromorphic model by presenting numerical calculations based on a linearized version of the finite-strain model and comparing the predictions to experimental results showing a marked size effect.

Key words: metallic foams, homogenization, polar-materials, microstructure, micromorphic, structured continua, solid mechanics, variational methods.

AMS 2000 subject classification: 74A35, 74A30, 74C05, 74C10 74C20, 74D10, 74E05, 74E10, 74E15, 74E20, 74G30, 74G65, 74N15

*Corresponding author: Patrizio Neff, AG6, Fachbereich Mathematik, Darmstadt University of Technology, Schlossgartenstrasse 7, 64289 Darmstadt, Germany, email: neff@mathematik.tu-darmstadt.de, Phone: 049-6151-163495

Contents

1 Introduction **3**
- 1.1 Theoretical aspects . . . 3
- 1.2 Application: continuum modelling of metallic foams. . . . 4

2 A finite-strain elastic micromorphic model with affine microstructure **5**
- 2.1 The elastic macroscopic micromorphic strain energy density . . . 7
- 2.2 The nonlinear elastic curvature energy density of the metallic foam . . . 7
- 2.3 The micromorphic balance equations . . . 8
- 2.4 The micromorphic micro-incompressible balance equations . . . 9
- 2.5 Constitutive consequences of the value for the Cosserat couple modulus . . . 9

3 Mathematical analysis **10**
- 3.1 Statement of the finite elastic micromorphic problem in variational form . . . 10
- 3.2 The external potentials . . . 11
- 3.3 The different cases . . . 12
- 3.4 Existence for the geometrically exact elastic micromorphic model . . . 12

4 The infinitesimal micromorphic elastic solid **15**
- 4.1 The variational formulation . . . 15
- 4.2 The linear system of balance equations . . . 16
- 4.3 Calculation of consistent effective elastic moduli . . . 16
- 4.4 Identification with Mindlin's representation . . . 18
- 4.5 The intrinsically linear micromorphic model . . . 19

5 Implementation **21**
- 5.1 Finite Element method for the infinitesimal micromorphic continuum . . . 21
- 5.2 Finite element simulations of hole size effects in metallic foams . . . 22

6 Final remarks **26**

7 Appendix **29**
- 7.1 Notation . . . 29
- 7.2 The coercivity inequality . . . 30
- 7.3 Derivation of the geometrically exact micromorphic balance equations . . . 30
- 7.4 Derivation of the geometrically exact micromorphic balance equations in the micro-incompressible case . . . 30
- 7.5 Validation of the Finite Element implementation . . . 32

1 Introduction

1.1 Theoretical aspects

This article addresses the modelling and mathematical analysis of **geometrically exact**[1] generalized continua of **micromorphic** type in the sense of Eringen in the elastic case. General continuum models involving **independent rotations** have already been introduced by the Cosserat brothers [19] at the beginning of the last century.

Their development has been largely forgotten for decades only to be rediscovered in the early sixties [64, 39, 1, 27, 25, 74, 75, 41, 56, 69, 76]. At that time theoretical investigations on non-classical continuum theories were the main motivation [51]. Since then, the Cosserat concept has been generalized in various directions, for an overview of these so called **microcontinuum** theories we refer to [26, 24, 8, 7, 9, 43, 53]. Recently, in [13, 14], the micromorphic balance equations derived by Eringen have been formally justified as a more realistic continuum model based on molecular dynamics and ensemble averaging.

The micromorphic model includes in a natural way **size effects**, i.e. small samples behave comparatively stiffer than large samples. These effects have recently received much attention in conjunction with nano-devices and cellular structures.

The mathematical analysis of general micromorphic solids in the static case is at present restricted to the infinitesimal, linear elastic models, see e.g. [46, 22, 44, 36, 37] for linear micropolar models and [49, 47, 48] for linear microstretch models. The major difficulty of the mathematical treatment in the finite-strain static case is related to the geometrically exact formulation of the theory and the appearance of **nonlinear manifolds** necessary for the description of the microstructure. In addition, **coercivity** turns out to be a delicate problem related to the possible **fracture** of the material. No general existence theorems for finite micromorphic models had been known until [60]. The simpler, geometrically exact nonlinear micropolar case has been dealt with in [61].

This contribution is organized as follows: first, in section 1.2 we motivate the application of the micromorphic model for the continuum-mechanical response of metallic foams. After that, we review (section 2) the basic concepts of the geometrically exact elastic micromorphic theories with affine microstructure in a variational context, i.e. we formulate the quasistatic conservative case as a minimization problem. For simplicity we restrict attention to a macroscopically physically linear stress-strain relation. Then we provide the corresponding balance equations and highlight the influence of material parameters on the ellipticity of the force balance equation.

More mathematically inclined readers may start directly in the analytical section 3. There, the complete problem statement of the geometrically exact elastic micromorphic case in a variational context is repeated. Since the **two-field** variational problem is only **conditionally coercive** we need to introduce a modification for the applied loads as given in [60] in order to ensure first that the functional to be minimized is bounded below and second that the curvature contribution can be controlled. This modification of the loads, herein called principle of **"bounded external work"**, expresses nothing but the physical fact that by moving a solid arbitrarily in a "real" force field only a finite amount of work can be gained. Such a condition is, however, unnecessary in either classical non-polar nonlinear/linear elasticity or the linear micromorphic model.

With this preparation existence of minimizers in suitable Sobolev-spaces is then established using the direct methods of variations and a novel extended Korn's first inequality. The mathematical development extends the development given in [60]. The investigation of the general micromorphic case with affine microstructure allows one to appreciate the peculiarities of the previously investigated micro-incompressible and micropolar subcases more closely. The special role played by the Cosserat couple modulus $\mu_c \geq 0$ is already seen in the infinitesimal strain case, where the two fields of deformation and microdeformation do not decouple even if $\mu_c = 0$.

Then we switch to the infinitesimal micromorphic elastic solid (section 4) for which we give the variational formulation (section 4.1) and the corresponding balance equations (section 4.2). Based on the linearized kinematics we determine effective material parameters in section 4.3 and provide an identification with the well known representation of Mindlin in section 4.4, ensuring automatically **positive definiteness** of the local strain energy.

In the final section 5 we compute the response of an infinite micromorphic continuum with a hole and identify it to the response of a cellular solid exhibiting strong size effects. We

[1] Fully frame-indifferent.

compare the response of a traditional Cosserat model and $\mu_c > 0$ with the response of the linear micromorphic model and $\mu_c = 0$. The relevant notation is introduced in the appendix. In the appendix we supply as well the coercivity inequality, the derivation of the nonlinear balance equations and an analytical solution for a simplified linear micromorphic boundary value problem.

1.2 Application: continuum modelling of metallic foams.

Cellular solids are strongly heterogeneous materials made of two highly contrasted constituents, namely air with the highest volume fraction and at least one ceramic, polymeric or metallic phase [38]. Their properties are extremely difficult to predict from the knowledge of the hard phase content since they strongly depend on the morphology of the hard skeleton. The complex microstructure of a nickel foam can be seen in figure 1 showing the distribution of open cells of characteristic size close to 500 μm. The edges of the faces of the polyhedral cells are nickel struts with a triangular cross–section.

The need for homogeneous effective models for the design of components and structures made of foam arises, because considering all individual cells remains computationally prohibitive. In principle, such homogeneous equivalent models can be obtained by means of classical homogenization techniques which are, however, difficult to extend to the extreme morphologies of cellular solids [42]. Alternatively, material parameters of phenomenological models can be identified from overall tensile curves or/and strain field measurements [4]. The substitution of such highly porous materials by a continuous homogeneous medium with an effective density, though necessary for practical applications, is rather challenging since many important features of the material behaviour can be lost. In particular, size effects are observed in metallic foams as a result of the interaction between the size of the considered structure and that of the microstructure, namely the cell size [63, 28, 6]. As a result, a continuum model should be able to reproduce, in a continuous way, the principle size effects. This is possible only if the phenomenological continuum model contains some constitutive intrinsic length scale(s) (here denoted by L_c). In particular, models based on classical Cauchy continua fail to reproduce the size effects presented in this work. The Cosserat continuum is a possible candidate for modelling cellular solids as recognized at several places [77, 67]. However, it will turn out to be quite inadequate when dealing with the size effect addressed in this work. The reason lies in the fact that cellular solids are highly compressible materials so that size effects do not merely arise from gradients of rotations (Cosserat approach) but also from microextension gradients [21]. That is why the attention is drawn here to the micromorphic continuum which is based on a full microdeformation tensor as additional degree of freedom. Another approach based on strain gradient plasticity was proposed in [11] for the modelling of size effects in sandwich beams containing aluminium foam.

We consider metallic foams mainly for their relatively high elastic stiffness in comparison to available polymer foams [38]. Even though the tensile curves of aluminium and nickel foams exhibit a clear elastic domain, the present work can only be seen as a prelude to more realistic nonlinear analyses within the framework of (finite-strain) elastoplasticity. Indeed, the size effect modeled in this work is not linked to a specific local constitutive behaviour of the metal struts. It can be rather seen as a benchmark test for the continuum medium chosen for representing a cellular solid.

We insist on the following prerequisite of the model for successful applications to structural computations. Let us consider a foam plate with a machined cylindrical hole of radius R and subject it to tensile loading, the load being applied far from the hole. If the cell size $l \ll R$, a simple classical continuum model is able to correctly predict the strain field around the hole. This has been demonstrated even in the nonlinear regime based on the comparison between Finite Element simulations and strain field measurements in a nickel foam [4]. Stress and strain concentrations occur at the equator where the crack leading to final fracture initiates.

However, when the hole size becomes close to the cell size, it is clear that such effect should not be noticeable any longer since the hole becomes nothing but a pore similar to the other ones. The transition from large hole behaviour up to the disappearance of any overall stress concentration effect in the case of holes with $R \sim l/2$, was studied experimentally by strain field measurements in [21].

A continuum model should be able to account for such a size effect if it is to be trusted for computing components containing holes and notches. We show in the computational part of the present work that the (infinitesimal) micromorphic model is able to reproduce at least

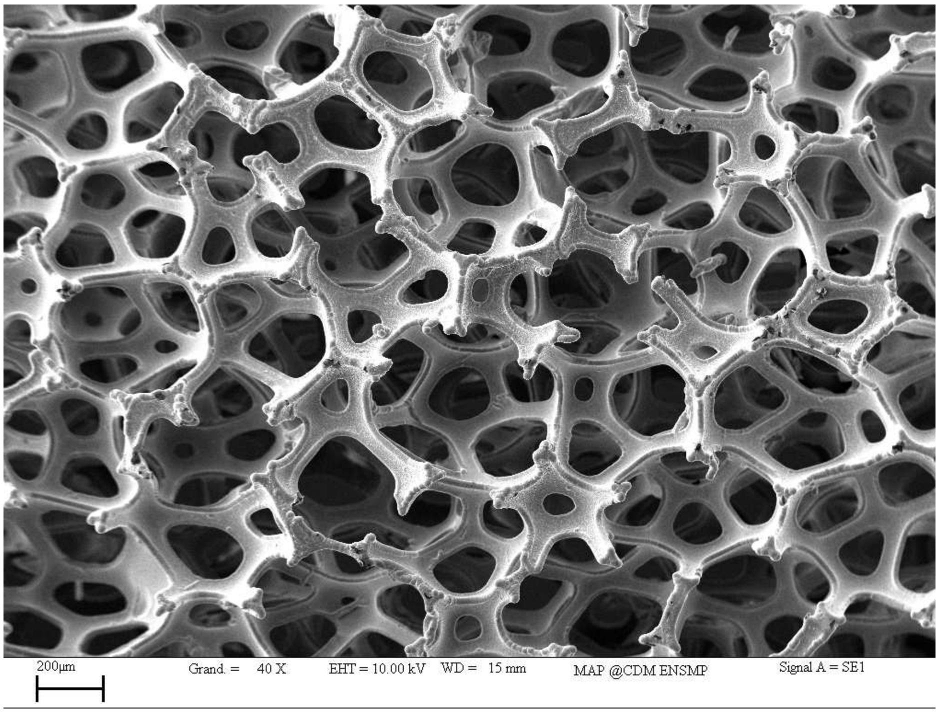

Figure 1: Scanning Electron Micrograph of a nickel foam for battery applications. The picture taken from [21] shows the distribution of cells and struts with characteristic sizes 500 μm and 70 μm respectively.

qualitatively this size effect, even in the elastic regime, by solving numerically the problem of a cylindrical hole in an infinite matrix. Furthermore, the numerical analysis provides a way of identifying the involved characteristic length.

2 A finite-strain elastic micromorphic model with affine microstructure

Let us now motivate a finite-strain micromorphic approach.[2] For our development we choose a strictly Lagrangean description. We first introduce an independent kinematical field of **microdeformations** $P \in \mathrm{GL}^+(3,\mathbb{R})$ together with its right polar decomposition

$$P = \overline{R}_p \cdot U_p = \mathrm{polar}(P) \cdot U_p = \overline{R}_p \, e^{\frac{\overline{\alpha}_p}{3}} \, \overline{U}_p \,, \quad \det[P] = e^{\overline{\alpha}_p} \,,$$
$$\overline{U}_p = \frac{U_p}{\det[U_p]^{1/3}} \in \mathrm{SL}(3,\mathbb{R}) \,, \quad \overline{P} = \frac{P}{\det[P]^{1/3}} \in \mathrm{SL}(3,\mathbb{R}) \,, \tag{2.1}$$

with $\overline{R}_p \in \mathrm{SO}(3,\mathbb{R})$ and $\overline{U_p} \in \mathrm{PSym}(3,\mathbb{R}) \cap \mathrm{SL}(3,\mathbb{R})$. The microdeformations P are meant to describe the substructure of the material which can **rotate**, **stretch**, **shear** and **shrink**. We refer to $\overline{R}_p$ as **microrotations**.

The micromorphic theory we deal with can formally be obtained by introducing the **multiplicative decomposition** of the macroscopic deformation gradient F into **independent microdeformation** P and the **micromorphic, nonsymmetric right stretch tensor** $\overline{U}$ (first Cosserat deformation tensor) with

$$F = P \cdot \overline{U} \,, \quad \overline{U} = P^{-1} F \,, \quad \overline{U} \in \mathrm{GL}^+(3,\mathbb{R}), \tag{2.2}$$

leading altogether to a **micro-compressible, micromorphic formulation**.[3]

---

[2] Following Eringen [24, p.13] we distinguish the **general micromorphic case**: $\overline{P} \in \mathrm{GL}^+(3,\mathbb{R}) = \mathbb{R}^+ \cdot \mathrm{SL}(3,\mathbb{R})$ with 9 additional **degrees of freedom** (dof); the **micro-incompressible micromorphic case**: $\overline{P} \in \mathrm{SL}(3,\mathbb{R})$ with 8 dof; the **microstretch case**: $\overline{P} \in \mathbb{R}^+ \cdot \mathrm{SO}(3,\mathbb{R})$ with 4 dof and the **micropolar case**: $\overline{P} \in \mathrm{SO}(3,\mathbb{R})$ with only 3 additional dof.

[3] The strain measure $\overline{U}$ which is induced by this definition corresponds to $\mathfrak{C}^T_{\mathrm{KL}}$ presented in (1.5.11)$_1$ of [24, p.15].

The notion **micro**morphic is prone to misunderstandings: the microdeformation P must be considered as a macroscopic (average) quantity as the deformation gradient and the resulting model is still phenomenological. However, geometrical features of the real substructure to be modelled determine the choice of geometric manifolds for P. Since the substructure of the metallic foam can in principle be crushed, the choice $P \in \mathrm{GL}^+(3,\mathbb{R})$ is mandatory.

In the **quasistatic** case, the micromorphic theory is derived from a **two-field** variational principle by postulating the following **"action euclidienne"** [19, p.156] I for the finite macroscopic deformation $\varphi : [0,T] \times \overline{\Omega} \mapsto \mathbb{R}^3$ and the independent microdeformation $P : [0,T] \times \overline{\Omega} \mapsto \mathrm{GL}^+(3,\mathbb{R})$:

$$
\begin{aligned}
I(\varphi, P) = \int_\Omega & W(F, P, \mathrm{D_x}P) - \Pi_f(\varphi) - \Pi_M(P)\,\mathrm{dV} \\
& - \int_{\Gamma_S} \Pi_N(\varphi)\,\mathrm{dS} - \int_{\Gamma_C} \Pi_{M_c}(P)\,\mathrm{dS} \mapsto \min\,.\ \text{w.r.t.}\ (\varphi, P), \\
P_{|_\Gamma} = P_{\mathrm{d}}\,, \quad & \varphi_{|_\Gamma} = g_{\mathrm{d}}(t)\,.
\end{aligned} \tag{2.3}
$$

The elastically stored energy density W depends on the macroscopic deformation gradient F as usual but in addition on the microdeformation P together with their first order space derivatives, represented through the third order tensor $\mathrm{D_x}P$. Here $\Omega \subset \mathbb{R}^3$ is a domain with boundary $\partial\Omega$ and $\Gamma \subset \partial\Omega$ is that part of the boundary, where Dirichlet conditions g, P_{d} for displacements and microdeformations, respectively, can be prescribed, while $\Gamma_S \subset \partial\Omega$ is a part of the boundary, where traction boundary conditions in the form of the potential of applied surface forces Π_N are given with $\Gamma \cap \Gamma_S = \emptyset$. The potential of external applied volume force is Π_f and Π_M takes on the role of the potential of applied external volume couples.[4] In addition, $\Gamma_C \subset \partial\Omega$ is the part of the boundary, where the potential of applied surface couples Π_{M_c} are applied with $\Gamma \cap \Gamma_C = \emptyset$. On the free boundary $\partial\Omega \setminus \{\Gamma \cup \Gamma_S \cup \Gamma_C\}$ corresponding natural boundary conditions for φ and P apply, which are obtained automatically in the variational process.

Variation of the action I with respect to φ yields the traditional equation for balance of linear momentum and variation of I with respect to P yields the additional balance of moment of momentum.

The standard conclusion from **frame-indifference** (here: invariance of the free energy under **s**uperposed **r**igid **b**ody **m**otions (**SRBM**) not merely **observer-invariance** of the model [73, 5, 57]: $\forall Q \in \mathrm{SO}(3,\mathbb{R}) : \quad W(F, P, \mathrm{D_x}P) = W(QF, QP, \mathrm{D_x}[QP])$ leads to the reduced representation of the energy (specify $Q = \overline{R}_p^T$):

$$
W(F, \overline{P}, \mathrm{D_x}P) = W(\overline{R}_p^T F, \overline{R}_p^T P, \overline{R}_p^T \mathrm{D_x}P) = W(U_p\overline{U}, U_p, \overline{R}_p^T \mathrm{D_x}P) = W^\sharp(\overline{U}, U_p, \mathfrak{K}_p, \nabla\overline{\alpha}_p)\,, \tag{2.4}
$$

where for $\overline{P} = \overline{R}_p\,\overline{U}_p \in \mathrm{SL}(3,\mathbb{R})$ we set

$$
\mathfrak{K}_p := \overline{R}_p^T \mathrm{D_x}\overline{P} = \left(\overline{R}_p^T \nabla(\overline{P}.e_1), \overline{R}_p^T \nabla(\overline{P}.e_2), \overline{R}_p^T \nabla(\overline{P}.e_3)\right) \in \mathbb{M}^{3\times3} \times \mathbb{M}^{3\times3} \times \mathbb{M}^{3\times3}\,, \tag{2.5}
$$

which coincides with one specific representation[5] of the third order right **micropolar curvature tensor** (or torsion-curvature tensor, wryness tensor, second Cosserat deformation tensor, bending-twist tensor, etc.), if $\overline{P} \in \mathrm{SO}(3,\mathbb{R})$.

For a geometrically exact (macroscopically isotropic) theory we assume in the following an additive split of the total free energy density into micromorphic local stretch (macroscopic), stretch of the substructure (microscopic) and micromorphic curvature part according to

$$
W^\sharp = \underbrace{W_{\mathrm{mp}}(\overline{U})}_{\text{macroscopic energy}} + \underbrace{W_{\mathrm{foam}}(\overline{U}_p, \overline{\alpha}_p)}_{\text{microscopic local energy}} + \underbrace{W_{\mathrm{curv}}(\mathfrak{K}_p, \nabla\overline{\alpha}_p)}_{\text{microscopic interaction energy}}\quad, \tag{2.6}
$$

[4] appearing in a non-mechanical context e.g. as influence of a magnetic field on the polarization of a substructure of the bulk.

[5] Note that $\mathfrak{K}_p^i = \overline{R_p}^T \nabla(\overline{P}.e_i) \notin \mathfrak{so}(3,\mathbb{R})$. Another representation of $\mathfrak{K}_p$ is given by $\overline{\mathfrak{K}}_p := \left(\overline{R}_p^T \partial_x \overline{P}, \overline{R}_p^T \partial_y \overline{P}, \overline{R}_p^T \partial_z \overline{P}\right) \in \mathfrak{T}(3)$. Since $\partial_x(\overline{R}_p^T \overline{P}) = 0$ for $\overline{P} = \overline{R}_p \in \mathrm{SO}(3,\mathbb{R})$, it holds that $\overline{\mathfrak{K}}_p \in \mathfrak{so}(3,\mathbb{R}) \times \mathfrak{so}(3,\mathbb{R}) \times \mathfrak{so}(3,\mathbb{R})$ in this case. It is therefore possible to base all considerations of curvature in the **micropolar** case on a more compact expression $\widehat{\mathfrak{K}}_p := \left(\mathrm{axl}(\overline{R}_p^T \partial_x \overline{R}_p) | \mathrm{axl}(\overline{R}_p^T \partial_y \overline{R}_p) | \mathrm{axl}(\overline{R}_p^T \partial_z \overline{R}_p)\right) \in \mathbb{M}^{3\times3}$. This is the traditional micropolar approach, see e.g. [68, 30, 40]. For us it is, however, not possible to use $\widehat{\mathfrak{K}}_p$, since we allow $\overline{P} \in \mathrm{GL}^+(3,\mathbb{R})$.

since a possible coupling between $\overline{U}$ and $\mathfrak{K}_p$ for centrosymmetric bodies can be ruled out [62, p.14].

2.1 The elastic macroscopic micromorphic strain energy density

For a macroscopic theory which is relevant mainly for **small elastic strain**[6] we require that $W_{\rm mp}(\overline{U})$ is a non-negative isotropic quadratic form (physically linear). This should cover already many cases of physical interest. We assume moreover the macroscopic stretch energy density normalized to

$$W_{\rm mp}(1\!\!1) = 0, \qquad D_{\overline{U}} W_{\rm mp}(\overline{U})_{|_{\overline{U}=1\!\!1}} = 0\,. \tag{2.7}$$

For the local energy contribution elastically stored in the cell-structure we assume the nonlinear expression

$$\begin{aligned} W_{\rm foam}(U_p) &= \underbrace{\mu^{\rm m}\,\|\frac{U_p}{\det[U_p]^{(1/3)}} - 1\!\!1\|^2}_{\text{isochoric substructure energy}} + \underbrace{\frac{\lambda^{\rm m}}{4}\left((\det[U_p]-1)^2 + (\frac{1}{\det[U_p]}-1)^2\right)}_{\text{volumetric energy}} \\ &= \mu^{\rm m}\,\|\overline{U}_p - 1\!\!1\|^2 + \frac{\lambda^{\rm m}}{4}\left((e^{\overline{\alpha}_p}-1)^2 + (e^{-\overline{\alpha}_p}-1)^2\right) =: W_{\rm foam}(\overline{U}_p, \overline{\alpha}_p)\,, \end{aligned} \tag{2.8}$$

avoiding self-interpenetration in a variational setting, since $W_{\rm foam} \to \infty$ as $\det[P] = \det[U_p] \to 0$ if $\lambda^{\rm m} > 0$.[7] The most general form of $W_{\rm mp}$ consistent[8] with the requirement (2.7) is

$$W_{\rm mp}(\overline{U}) = \mu_e\,\|\,{\rm sym}(\overline{U} - 1\!\!1)\|^2 + \mu_c\,\|\,{\rm skew}(\overline{U} - 1\!\!1)\|^2 + \frac{\lambda_e}{2}\,{\rm tr}\left[{\rm sym}(\overline{U} - 1\!\!1)\right]^2, \tag{2.9}$$

with material constants μ_e, μ_c, λ_e such that $\mu_e,\ 3\lambda_e + 2\mu_e, \mu_c \geq 0$ from non-negativity [24] of (2.9). **It is important to realize that μ_e, λ_e are effective elastic constants which in general do not coincide with the classical Lamé constants $\mu, \lambda > 0$.** Here, we take the classical Lamé constants to be obtained from standard experiments of sufficiently large samples of the materials, such that length scale effects do not interfere. The so-called **Cosserat couple modulus** μ_c (rotational couple modulus) remains for the moment unspecified, but we note that $\mu_c = 0$ is physically possible, since the **micromorphic reaction stress** $D_{\overline{U}} W_{\rm mp}(\overline{U}) \cdot \overline{U}^T$ is not symmetric in general, i.e. the problem does not decouple. For comparison, in [24, p.111] for the infinitesimal micropolar case, the elastic moduli are taken to be $\mu_e = \mu + \frac{\kappa}{2}$, $\mu_c = \frac{\kappa}{2}$, $\lambda_e = \lambda$, but in this formula μ can neither be regarded as one of the Lamé constants.[9] [10] In [20, 71, 72, 31, 23, 32] the abbreviation μ_c is used while in [40] it is $\mu_c = \alpha$ and $\mu_c = G_c$ in [50] for the micropolar theory.

By formal similarity with the classical formulation, we may call $\mu^{\rm m}, \lambda^{\rm m}$ the **microscopic Lamé moduli** of the affine substructure, which can in principle be determined from classical experiments or numerical computation on the microscale, e.g. dealing with a nickel-foam structure, they are the Lamé-constants of the smallest possible representative volume element (RVE) in the foam. In section 4.3 it will be shown how to obtain consistent values for μ_e, λ_e if we know already the microscopic values $\mu^{\rm m}, \lambda^{\rm m}$ and the macroscopic constants μ, λ.

2.2 The nonlinear elastic curvature energy density of the metallic foam

The curvature energy is responsible for the size-dependent resistance of the cell-structure against local twisting and inhomogeneous volume change. Thus inhomogeneous microstructural rear-

[6] By this we mean that the part of the deformation which is superposed onto the substructure deformation has small elastic strains.

[7] Note that $\left((\det[U_p]-1)^2 + (\frac{1}{\det[U_p]}-1)^2\right) = 2\,{\rm tr}\left[U_p - 1\!\!1\right]^2 + O(\|U_p - 1\!\!1\|^3)$.

[8] Mixed products like $\langle \overline{U} - 1\!\!1, \overline{U}_p - 1\!\!1\rangle$ and ${\rm tr}\left[\overline{U} - 1\!\!1\right] \cdot {\rm tr}\left[\overline{U}_p - 1\!\!1\right]$ are excluded by non-negativity.

[9] A simple definition of the Lamé constants in (the restricted case of) micropolar elasticity is that they should coincide with the classical Lamé constants for symmetric situations. Equivalently, they are obtained by the classical formula $\mu = \frac{E}{2(1+\nu)}$, $\lambda = \frac{E\nu}{(1+\nu)(1-2\nu)}$, where E and ν are uniquely determined from uniform traction experiments for sufficiently large samples.

[10] Uniform traction and uniform compression do not activate rotations, hence the classical identification of the Lamé constants is achieved **independent** of μ_c. Uniform traction alone allows to determine the Young modulus E and the Poisson ratio ν [17, p.126]. Contrary to [34, p.411] we do not see the possibility to define a specific "micropolar Young modulus" or "micropolar Poisson ratio".

rangements are penalized. For the curvature term, to be specific, we assume the general form

$$W_{\text{curv}}(\mathfrak{K}_p, \nabla\overline{\alpha}_p) = \mu \frac{L_c^{1+p}}{12} \left(1 + \alpha_4 L_c^q \|\mathfrak{K}_p\|^q\right) \left(\alpha_5 \|\operatorname{sym}\mathfrak{K}_p\|^2 + \alpha_6 \|\operatorname{skew}\mathfrak{K}_p\|^2 + \alpha_7 \operatorname{tr}[\mathfrak{K}_p]^2\right)^{\frac{1+p}{2}}$$
$$+ \mu \frac{L_c^{1+p}}{12} \left(\alpha_8 \|\nabla\overline{\alpha}_p\|^{1+p} + \alpha_8 L_c \|\nabla\overline{\alpha}_p\|^{2+p}\right), \tag{2.10}$$

where $L_c > 0$ is setting an internal length scale with units of length. It is to be noted that we have decoupled the curvature coming from inhomogeneous volume changes and from pure twisting. The values $\alpha_4 \geq 0, p > 0$ and $q \geq 0$ are additional material constants. The factor $\frac{1}{12}$ appears only for convenience and $\alpha_5 > 0, \alpha_6, \alpha_7 \geq 0, \alpha_8 > 0$ should be satisfied as a minimal requirement. We mean $\operatorname{tr}[\mathfrak{K}_p]^2 = \|\operatorname{tr}[\mathfrak{K}_p]\|^2$ by abuse of notation. This choice for W_{curv} does not presuppose any knowledge of the magnitude of the micromorphic curvature in the material and is non-degenerate in the origin $\|\mathfrak{K}_p\| = 0,\ \|\nabla\overline{\alpha}_p\| = 0$.

Some care has to be exerted in the finite-strain regime: W_{curv} should preferably be **coercive** in the sense that we impose pointwise

$$\exists\, c^+ > 0\ \exists\, r > 1 :\ \forall\, \mathfrak{K}_p \in \mathfrak{T}(3)\ \forall \xi \in \mathbb{R}^3 : \quad W_{\text{curv}}(\mathfrak{K}_p, \xi) \geq c^+ \|(\mathfrak{K}_p, \xi)\|^r, \tag{2.11}$$

or less demanding

$$\exists\, r > 1 : \quad \frac{W_{\text{curv}}(\mathfrak{K}_p, \xi)}{\|(\mathfrak{K}_p, \xi)\|^r} \to \infty \quad \text{as } \|(\mathfrak{K}_p, \xi)\| \to \infty, \tag{2.12}$$

which implies necessarily $\alpha_6,\ \alpha_8 > 0$ in (2.10). Observe that our formulation of the micromorphic curvature tensor is mathematically convenient in the sense that $\|\mathfrak{K}_p\| = \|\overline{R}_p^T \mathrm{D_x}\overline{P}\| = \|\mathrm{D_x}\overline{P}\|$ provides pointwise control of all first derivatives of $\overline{P}$ independent of the values of $\overline{P}$ itself.[11]

Note that the presented formulation still includes a finite Cosserat micropolar model as a special case, if we set $\overline{P} = \overline{R} \in \mathrm{SO}(3,\mathbb{R})$. In this fashion, we have the following correspondence of limit problems:

$$\begin{aligned}
\lambda^{\mathrm{m}} \to \infty \quad &\Rightarrow \quad \textbf{micro-incompressible model: manifold } \mathrm{SL}(3,\mathbb{R}),\\
\mu^{\mathrm{m}} \to \infty \quad &\Rightarrow \quad \textbf{microstretch model: manifold } \mathbb{R}^+ \cdot \mathrm{SO}(3,\mathbb{R}),\\
\mu^{\mathrm{m}}, \lambda^{\mathrm{m}} \to \infty \quad &\Rightarrow \quad \textbf{micropolar model: manifold } \mathrm{SO}(3,\mathbb{R}),\\
\mu^{\mathrm{m}}, \lambda^{\mathrm{m}}, \mu_c \to \infty \quad &\Rightarrow \quad \textbf{higher (second) gradient continua}.
\end{aligned} \tag{2.13}$$

2.3 The micromorphic balance equations

For the choices we have made we supply the resulting material form of the highly nonlinear field equations on the reference configuration (with $\alpha_4 = 0,\ p = 1$) which can be obtained after some algebraic manipulations, see section 7.3 (We have gathered the influence of the external potentials in $\Pi(x, \varphi, P)$):

$$0 = \operatorname{Div}\left(S_1(F,P) + 2\,\mu_c\, P^{-T} \operatorname{skew}(P^{-1}F)\right) + D_\varphi \Pi(x, \varphi(x), P)_{\mathbb{R}^3}, \quad \textbf{balance of forces},$$
$$0 = \operatorname{skew}(\overline{U}_p^{-1} D_{\overline{U}} W_{\text{mp}}(\overline{U})\, \overline{U}^T \overline{U}_p^T) + \operatorname{skew}\left(\overline{R}_p^T \operatorname{Div}\left[\overline{R}_p\, D_{\mathfrak{K}_p} W_{\text{curv}}(\mathfrak{K}_p, \nabla\overline{\alpha}_p)\right] \overline{U}_p\right)$$
$$+ \operatorname{skew}\left(D_{\mathfrak{K}_p} W_{\text{curv}}(\mathfrak{K}_p, \nabla\overline{\alpha}_p)\mathfrak{K}_p^T\right) + \operatorname{skew}\left(\overline{R}_p^T D_{\overline{P}} \Pi(x, \varphi(x), P) \overline{U}_p\right)_{\mathbb{M}^{3\times3}},$$
$$\textbf{rotational momentum},$$
$$0 = \operatorname{dev}\operatorname{sym}\left(\overline{U}_p^{-1} D_{\overline{U}} W_{\text{mp}}(\overline{U})\, \overline{U}^T \overline{U}_p^T\right) - \operatorname{dev}\operatorname{sym}\left(D_{\overline{U}_p} W_{\text{foam}}(\overline{U}_p, \overline{\alpha}_p)\, \overline{U}_p^T\right) \tag{2.14}$$
$$+ \operatorname{dev}\operatorname{sym}\left(\overline{R}_p^T \operatorname{Div}\left[\overline{R}_p\, D_{\mathfrak{K}_p} W_{\text{curv}}(\mathfrak{K}_p, \nabla\overline{\alpha}_p)\right] \overline{U}_p\right) + \operatorname{dev}\operatorname{sym}\left(\overline{R}_p^T D_{\overline{P}} \Pi(x, \varphi(x), P) \overline{U}_p\right),$$
$$\textbf{volumetric momentum},$$
$$0 = \operatorname{tr}\left[\overline{U}_p^{-1} D_{\overline{U}} W_{\text{mp}}(\overline{U})\, \overline{U}^T \overline{U}_p^T\right] - D_{\overline{\alpha}_p} W_{\text{foam}}(\overline{U}_p, \overline{\alpha}_p) + \operatorname{Div} D_{\nabla\overline{\alpha}_p} W_{\text{curv}}(\mathfrak{K}_p, \nabla\overline{\alpha}_p), \tag{2.15}$$
$$\textbf{isochoric momentum},$$

[11] This is not true for other possible basic invariant curvature expressions like $\overline{P}^{-1}\mathrm{D_x}\overline{P}$ or $\overline{P}^T\mathrm{D_x}\overline{P}$ or $F^T\mathrm{D_x}\overline{P}$, see Eringen [24, 1.5.4,1.5.11].

where S_1 is the first Piola-Kirchhoff stress (for $\mu_c = 0$) with the functional form

$$S_1(F, P) = P^{-T} \left[2\,\mu\, \mathrm{sym}\left(P^{-1}F - 1\!\!1\right) + \lambda\, \mathrm{tr}\left[P^{-1}F - 1\!\!1\right] 1\!\!1\right] , \tag{2.16}$$

similar to [59, (P3)] and $D_{\mathfrak{K}_p} W_{\mathrm{curv}}(\mathfrak{K}_p)$ is the material **micromorphic moment tensor** (or **couple-stress tensor**). Note that $D_{\overline{R}_p} W_{\mathrm{foam}}(\overline{U}_p, \overline{\alpha}_p) = 0$, leaving no contribution of the local foam energy in the rotational momentum equation.

In our subsequent variationally based mathematical development the nonlinear balance equations will not play a prominent role. They become more important, however, for our numerical calculations.

Remark 2.1
Observe the chain of symmetry conditions for isochoric macroscopic relative elastic strain energies $W_{\mathrm{mp}}(\overline{U})$:

$$\begin{aligned}
&\overline{U} \in \mathrm{Sym} \Rightarrow \quad D_{\overline{U}} W_{\mathrm{mp}}(\overline{U}) \in \mathrm{Sym} \Rightarrow \quad D_{\overline{U}} W_{\mathrm{mp}}(\overline{U})\, \overline{U}^T \in \mathrm{Sym} \Leftrightarrow S_2(F, P) \in \mathrm{Sym}\,, \\
&\quad S_2(F, P) := F^{-1} D_F W_{\mathrm{mp}}(P^{-1}F) \in \mathrm{Sym}\,.
\end{aligned} \tag{2.17}$$

The reverse implications are in general false.

2.4 The micromorphic micro-incompressible balance equations

In the special case $P = \overline{P} \in \mathrm{SL}(3, \mathbb{R})$, $\overline{\alpha}_p \equiv 0$, the balance equations have to incorporate the nonlinear constraint $\det[P] \equiv 1$. This can be done by suitably restricting the possible variations of P, see (7.6) and set $W_{\mathrm{foam}}(\overline{U}_p) := W_{\mathrm{foam}}(\overline{U}_p, 0)$

$$\begin{aligned}
0 &= \mathrm{Div}\left[\left(S_1(F, \overline{P}) + 2\,\mu_c\, \overline{P}^{-T} \mathrm{skew}(\overline{P}^{-1} F)\right)\right] + D_\varphi \Pi(x, \varphi(x), \overline{P})_{\mathbb{R}^3}\,, \\
0 &= \mathrm{skew}(\overline{U}_p^{-1} D_{\overline{U}} W_{\mathrm{mp}}(\overline{U})\, \overline{U}^T \overline{U}_p^T) + \mathrm{skew}\left(\overline{R}_p^T\, \mathrm{Div}\left[\overline{R}_p\, D_{\mathfrak{K}_p} W_{\mathrm{curv}}(\mathfrak{K}_p)\right] \overline{U}_p\right) \\
&\quad + \mathrm{skew}\left(D_{\mathfrak{K}_p} W_{\mathrm{curv}}(\mathfrak{K}_p) \mathfrak{K}_p^T\right) + \mathrm{skew}\left(\overline{R}_p^T D_{\overline{P}} \Pi(x, \varphi(x), \overline{P}) \overline{U}_p\right)_{\mathbb{M}^{3\times 3}}\,, \\
0 &= \mathrm{dev\,sym}\left(\overline{U}_p^{-1} D_{\overline{U}} W_{\mathrm{mp}}(\overline{U})\, \overline{U}^T \overline{U}_p^T\right) - \mathrm{dev\,sym}\left(D_{\overline{U}_p} W_{\mathrm{foam}}(\overline{U}_p)\, \overline{U}_p^T\right) \\
&\quad + \mathrm{dev\,sym}\left(\overline{R}_p^T\, \mathrm{Div}\left[\overline{R}_p\, D_{\mathfrak{K}_p} W_{\mathrm{curv}}(\mathfrak{K}_p)\right] \overline{U}_p\right) + \mathrm{dev\,sym}\left(\overline{R}_p^T D_{\overline{P}} \Pi(x, \varphi(x), \overline{P}) \overline{U}_p\right)\,.
\end{aligned} \tag{2.18}$$

A similar form of the unconventional[12] balance of angular momentum equation has been given in [7, p.63] for the micropolar case.

2.5 Constitutive consequences of the value for the Cosserat couple modulus

Looking at (2.9) with $\mu_c > 0$ we see that the implication of this choice for μ_c at a first glance is an innocuous rise in the macroscopic elastic strain energy $W_{\mathrm{mp}}(\overline{U})$, if $\overline{R}_p \neq \mathrm{polar}(F)$, but $\overline{R}_p$ is generically assumed to be independent of the continuum rotations polar(F). The choice $\mu_c > 0$ acts like a local "elastic spring" between both continuum rotations and microrotations.

Let us consider the mathematical implications of $\mu_c = 0$ and $0 < \mu_c \leq \mu$, respectively, in more detail. It is readily verified that for the elasticity tensors (differentiating the stretch energy density $W_{\mathrm{mp}}(\overline{U})$ at fixed P w.r.t. F)

$$\begin{aligned}
\mu_{\mathbf{c}} > 0 :\ \forall\, H \in \mathbb{M}^{3\times 3} &: D_F^2 W_{\mathrm{mp}}(P^{-1}F).(H, H) \geq 2\,\mu_c\, \|P^{-1}H\|^2 \geq 2\mu_c\, \lambda_{\min}(P^{-T}P^{-1})\, \|H\|^2, \\
\mu_{\mathbf{c}} = 0 :\ \forall\, H \in \mathbb{M}^{3\times 3} &: D_F^2 W_{\mathrm{mp}}(P^{-1}F).(H, H) \geq 2\,\mu\, \|\frac{1}{2}(P^{-1}H + H^T P^{-T})\|^2\,.
\end{aligned} \tag{2.19}$$

[12] Since we have not transformed the tensor equation into a related vector format, which is usually preferred in the micropolar case. Following [7] we can identify an external volume couple b_c in the equilibrium vector-format with $\mathrm{axl}(\mathrm{skew}(\overline{R}_p^T M))$. Then b_c is a volume couple which is not a dead load. We note that a term $\mathrm{skew}\left(D_{\mathfrak{K}_p} W_{\mathrm{curv}}(\mathfrak{K}_p)\, \mathfrak{K}_p^T\right)$ does not directly appear in derivations based on $\widehat{\mathfrak{K}}_p$ since e.g. $\widehat{\mathfrak{K}}_p^1 = \mathrm{axl}(\overline{R}_p^T \partial_x \overline{R}_p)$ and variation along a one-parameter group of rotations yields

$$\delta \widehat{\mathfrak{K}}_p^1 = \mathrm{axl}((A\overline{R}_p)^T \partial_x \overline{R}_p + \overline{R}_p^T \partial_x [A\overline{R}_p]) = \mathrm{axl}(-\overline{R}_p^T A \partial_x \overline{R}_p + \overline{R}_p^T (\partial_x A) \overline{R}_p + \overline{R}_p^T A \partial_x \overline{R}_p) = \mathrm{axl}(\overline{R}_p^T (\partial_x A) \overline{R}_p)\,.$$

This is not at variance with $(2.18)_2$ since differentiation is carried out differently. Observe that $\mathrm{skew}\left(D_{\mathfrak{K}_p} W_{\mathrm{curv}}(\mathfrak{K}_p)\, \mathfrak{K}_p^T\right) = 0$ if $\alpha_5 = \alpha_6$, $\alpha_7 = 0$, i.e. if couple stresses are proportional to the curvature tensor.

Hence the choice $\mu_c > 0$ leads to **uniform convexity** of $W_{\mathrm{mp}}(P^{-1}F)$ w.r.t. F if $P \in L^\infty(\Omega, \mathrm{GL}^+(3,\mathbb{R}))$ and **unconditional elastic stability** on the macroscopic level: regardless of what spatial distribution of microdeformations $P(x)$ is given, the macroscopic equation of balance of linear momentum would then be uniquely solvable and this equation is insensitive to any deterioration of the spatial features of the microstructure as long as P is merely essentially bounded. Uniform convexity is difficult to accept from a constitutive point of view, since uniform convexity is impossible for a geometrically exact description in the framework of a classical macroscopic continuum but clear from the above discussion: the additional elastic spring between micro- and continuum rotation extremely rigidifies the material and completely changes the type of the mathematical boundary value problem in comparison with the classical finite elasticity theory.

Fortunately, such a far reaching unsatisfactory conclusion does not hold for zero Cosserat couple modulus $\mu_c = 0$, in which case we have for $\xi, \eta \in \mathbb{R}^3$:

$$\begin{aligned} D_F^2 W_{\mathrm{mp}}(P^{-1}F).(\xi\otimes\eta, \xi\otimes\eta) &= \mu\big(\|P^{-1}\xi\otimes\eta\|^2 + \langle P^{-1}\xi\otimes\eta, \eta\otimes P^{-1}\xi\rangle\big) \\ &= \mu\Big(\|P^{-1}\xi\otimes\eta\|^2 + \langle P^{-1}\xi, \eta\rangle^2\Big) \geq \mu\,\|P^{-1}\xi\otimes\eta\|^2, \end{aligned} \tag{2.20}$$

which shows the physically much more appealing inequality

$$D_F^2 W_{\mathrm{mp}}(P^{-1}F).(\xi\otimes\eta, \xi\otimes\eta) \geq \mu\,\lambda_{\min}(P^{-T}P^{-1})\,\|\xi\|^2\cdot\|\eta\|^2\,, \tag{2.21}$$

expressing nothing but **uniform Legendre-Hadamard ellipticity** of the acoustic-tensor with ellipticity constant $\mu\,\lambda_{\min}(P^{-T}P^{-1})$. As a result we see that **for large microstructural expansion P, the ellipticity constant may deteriorate, i.e. the larger the foam is extended, the weaker it gets while the compressed metallic foam gets stiffer**. The Legendre-Hadamard condition has the most convincing physical basis [2, p.461] because it implies the **reality of wave speeds** and the **Baker-Ericksen inequalities** (stress increases with strain, [52, p.19]).[13]

3 Mathematical analysis

3.1 Statement of the finite elastic micromorphic problem in variational form

Let us gather the obtained three-field problem posed in a variational form. The task is to find a triple $(\varphi, \overline{P}, \overline{\alpha}_p) : \Omega \subset \mathbb{R}^3 \mapsto \mathbb{R}^3 \times \mathrm{SL}(3,\mathbb{R}) \times \mathbb{R}$ of **macroscopic** deformation φ and **independent microdeformation** $P = e^{\frac{\overline{\alpha}_p}{3}}\,\overline{P}$, minimizing the energy functional I with

$$\begin{aligned} I(\varphi, \overline{P}, \overline{\alpha}_p) = \int_\Omega W_{\mathrm{mp}}(P^{-1}\nabla\varphi) + W_{\mathrm{foam}}(\overline{U}_p, \overline{\alpha}_p) + W_{\mathrm{curv}}(\overline{R}_p^T \mathrm{D_x}\overline{P}, \nabla\overline{\alpha}_p) - \Pi_f(\varphi) - \Pi_M(P)\,\mathrm{dV} \\ - \int_{\Gamma_S}\Pi_N(\varphi)\,\mathrm{dS} - \int_{\Gamma_C}\Pi_{M_c}(P)\,\mathrm{dS} \mapsto \min.\ \text{w.r.t. } (\varphi, \overline{P}, \overline{\alpha}_p), \end{aligned} \tag{3.1}$$

under the constraints

$$\overline{U}_p = \overline{R}_p^T\overline{P}, \quad \overline{R}_p = \mathrm{polar}(\overline{P}), \quad \overline{U} = P^{-1}\nabla\varphi\,, \quad P = e^{\frac{\overline{\alpha}_p}{3}}\,\overline{P}\,, \tag{3.2}$$

and the Dirichlet boundary conditions

$$\varphi_{|_\Gamma} = g_{\mathrm{d}}\,, \qquad \overline{R}_{p_{|_\Gamma}} = \overline{R}_{p_{\mathrm{d}}}, \quad \overline{U}_{p_{|_\Gamma}} = \overline{U}_{p_{\mathrm{d}}} \Rightarrow \overline{P}_{|_\Gamma} = \overline{R}_{p_{\mathrm{d}}}\overline{U}_{p_{\mathrm{d}}}\,, \quad \overline{\alpha}_{p_{|_\Gamma}} = \overline{\alpha}_{p_{\mathrm{d}}}\,. \tag{3.3}$$

[13] The preferred value $\mu_c = 0$ for the macroscopic case can as well be motivated by the following consideration: Consider the Green strains $F^TF - 1\!\!1 = (\overline{U} - 1\!\!1)^T(\overline{U} - 1\!\!1) + 2\,\mathrm{sym}(\overline{U} - 1\!\!1)$. Therefore $\frac{\mu}{4}\|F^TF - 1\!\!1\|^2 = \mu\|\,\mathrm{sym}\,\overline{U} - 1\!\!1\|^2 + O(\|\overline{U} - 1\!\!1\|^3)$. Hence $\mu_c = 0$ provides the correct first order approximation to a classical St. Venant-Kirchhoff material. With $\mu_c = 0$ we exclusively recover the fact of the classical continuum theory that W isotropic implies symmetry of the Biot stress tensor: $D_{\overline{U}}W(\overline{U}) \in \mathrm{Sym}$. If we expand $\overline{R} = 1\!\!1 + \overline{A} + \dots$ with $\overline{A} \in \mathfrak{so}(3)$ and write $F = 1\!\!1 + \nabla u$, then the micropolar effects disappear to first order for $\mu_c = 0$. In this sense, $\mu_c = 0$ is close to classical elasticity.

Here, the constitutive assumptions on the densities are taken to be

$$
\begin{aligned}
W_{\mathrm{mp}}(\overline{U}) &= \mu_e \, \|\operatorname{sym}(\overline{U}-\mathbb{1})\|^2 + \mu_c \, \|\operatorname{skew}(\overline{U})\|^2 + \frac{\lambda_e}{2} \operatorname{tr}\left[\operatorname{sym}(\overline{U}-\mathbb{1})\right]^2 , \\
W_{\mathrm{foam}}(\overline{U}_p, \overline{\alpha}_p) &= \mu^{\mathrm{m}} \, \|\overline{U}_p - \mathbb{1}\|^2 + \frac{\lambda^{\mathrm{m}}}{4} \, \left((e^{\overline{\alpha}_p}-1)^2 + (e^{-\overline{\alpha}_p}-1)^2\right) , \qquad (3.4) \\
W_{\mathrm{curv}}(\mathfrak{K}_p, \nabla\overline{\alpha}_p) &= \mu \frac{L_c^{1+p}}{12} \, (1 + \alpha_4 \, L_c^q \, \|\mathfrak{K}_p\|^q) \left(\alpha_5 \, \|\operatorname{sym}\mathfrak{K}_p\|^2 + \alpha_6 \, \|\operatorname{skew}\mathfrak{K}_p\|^2 + \alpha_7 \operatorname{tr}\left[\mathfrak{K}_p\right]^2\right)^{\frac{1+p}{2}} \\
&\quad + \mu \frac{L_c^{1+p}}{12} \mu \, \left(\alpha_8 \|\nabla\overline{\alpha}_p\|^{1+p} + \alpha_8 \, L_c \, \|\nabla\overline{\alpha}_p\|^{2+p}\right) , \\
\mathfrak{K}_p &= \overline{R}_p^T \mathrm{D_x} \overline{P} = \left(\overline{R}_p^T \nabla(\overline{P}.e_1), \overline{R}_p^T \nabla(\overline{P}.e_2), \overline{R}_p^T \nabla(\overline{P}.e_3)\right), \text{the third order } \textbf{curvature tensor} .
\end{aligned}
$$

The total elastically stored energy $W = W_{\mathrm{mp}} + W_{\mathrm{foam}} + W_{\mathrm{curv}}$ depends on the deformation gradient $F = \nabla\varphi$, and the microdeformations P together with their space derivatives. Here $\Omega \subset \mathbb{R}^3$ is a domain with boundary $\partial\Omega$ and $\Gamma \subset \partial\Omega$ is that part of the boundary, where Dirichlet conditions $g_{\mathrm{d}}, P_{\mathrm{d}}$ for displacements and microdeformations, respectively, are prescribed, while $\Gamma_S \subset \partial\Omega$ is a part of the boundary, where traction boundary conditions in the form of the potential of applied surface forces Π_N are given with $\Gamma \cap \Gamma_S = \emptyset$. In addition, $\Gamma_C \subset \partial\Omega$ is the part of the boundary where the potential of external surface couples Π_{M_c} are applied with $\Gamma \cap \Gamma_C = \emptyset$. On the free boundary $\partial\Omega \setminus \{\Gamma \cup \Gamma_S \cup \Gamma_C\}$ corresponding natural boundary conditions for (φ, P) apply. The potential of the external applied volume force is Π_f and Π_M takes on the role of the potential of applied external volume couples.

The parameters μ_e, $\lambda_e > 0$ govern the **relative elastic deformation**, $\mu_c \geq 0$ is called the **Cosserat couple modulus**, μ^{m}, $\lambda^{\mathrm{m}} > 0$ are the Lamé constants of a representative volume element (RVE) of the substructure and $L_c > 0$ introduces an **internal length** which is **characteristic** for the material, e.g. related to the cell size of the metallic foam. The parameters α_i, $i = 1,..,8$ are dimensionless weighting factors. If not stated otherwise, we assume that $\alpha_5 > 0, \alpha_6 > 0, \alpha_8 > 0, \alpha_7 \geq 0$.

A finite Cosserat micropolar theory is included in the formulation (3.1),(3.2),(3.4) by restricting it to $\overline{P} \in \mathrm{SO}(3,\mathbb{R})$ or setting $\mu^{\mathrm{m}}, \lambda^{\mathrm{m}} = \infty$, formally. Similarly, for $\mu^{\mathrm{m}} = \infty$ only we recover the micro-stretch formulation with $\overline{P} \in \mathbb{R}^+ \cdot \mathrm{SO}(3,\mathbb{R})$ and for $\lambda^{\mathrm{m}} = \infty$, we recover the micro-incompressible formulation case $\overline{P} \in \mathrm{SL}(3,\mathbb{R})$.

3.2 The external potentials

Traditionally, in the conservative, dead load case one would have

$$
\Pi_f(\varphi) = \langle f, \varphi \rangle , \quad \Pi_M(\overline{P}) = \langle M, P \rangle , \quad \Pi_N(\varphi) = \langle N, \varphi \rangle , \quad \Pi_{M_c}(P) = \langle M_c, P \rangle , \qquad (3.5)
$$

for the potentials of applied loads with given functions $f \in L^2(\Omega, \mathbb{R}^3)$, $M \in L^2(\Omega, \mathbb{M}^{3\times3})$, $N \in L^2(\Gamma_S, \mathbb{R}^3)$, $M_c \in L^2(\Gamma_C, \mathbb{M}^{3\times3})$.

For our treatment, we need to assume, however, that the external potentials, describing the configuration dependent applied loads, are continuous with respect to the topology of $L^1(\Omega)$, $L^1(\Gamma_S)$, $L^1(\Gamma_C)$, respectively and satisfy in addition the condition

$$
\begin{aligned}
&\exists\, C^+ > 0 \quad \forall\, \varphi \in L^1(\Omega, \mathbb{R}^3),\; P \in L^1(\Omega, \mathrm{GL}^+(3,\mathbb{R})) \;: \\
&\qquad \int_\Omega \Pi_f(\varphi) - \Pi_M(P)\, \mathrm{dV}, \quad \int_{\Gamma_S} \Pi_N(\varphi)\, \mathrm{dS}, \quad \int_{\Gamma_C} \Pi_{M_c}(P)\, \mathrm{dS} \leq C^+ . \qquad (3.6)
\end{aligned}
$$

While continuity is satisfied e.g. for the dead load case $\Pi_f(\varphi) = \langle f, \varphi \rangle$ and $f \in L^\infty(\Omega)$, the second condition (3.6) restricts attention to **"bounded external work"**. If we want to describe a situation corresponding to the classical dead load case, we could take

$$
\Pi_f(\varphi) = \frac{1}{1 + [\|\varphi(x)\| - K^+]_+} \, \langle f(x), \varphi(x) \rangle , \qquad (3.7)
$$

for some large positive constant K^+ and $[\cdot]_+$ the positive part of a scalar argument. It suffices now that $f \in L^1(\Omega)$, then $\int_\Omega \Pi_f(\varphi)\, \mathrm{dV} \leq C^+$, independent of $\varphi \in L^1(\Omega)$.

The new condition (3.6) can be rephrased as saying that only a finite amount of work can be performed against the external loads, regardless of the magnitude of translation and microdeformation. This is certainly true for any real field of applied loads.[14]

[14] In classical finite elasticity, such a condition is not necessary, since the elastic energy density is assumed a

3.3 The different cases

We distinguish three different situations:

I: $\mu_c > 0$, $\alpha_4 \geq 0$, $p \geq 1$, $q \geq 0$, elastic macro-stability, local first order micromorphic. **Fracture excluded**.

II: $\mu_c = 0$, $\alpha_4 > 0$, $p \geq 1$, $q > 1$, elastic pre-stability, nonlocal second order micromorphic, macroscopic specimens, in a sense close to classical elasticity, zero Cosserat couple modulus. **Fracture excluded**.

III: $\mu_c = 0$, $\alpha_4 = 0$, $0 < p \leq 1$, $q = 0$, elastic pre-stability, nonlocal second order micromorphic theory, macroscopic specimens, in a sense close to classical elasticity, zero Cosserat couple modulus. Since possibly $\varphi \notin W^{1,1}(\Omega, \mathbb{R}^3)$, due to lack of elastic coercivity, **including fracture** in multiaxial situations.

We refer to $0 < p < 1$, $q \geq 0$ as the **sub-critical case**, to $p = 1$, $q \geq 0$ as the **critical case** and to $p \geq 1$, $q > 1$ as the **super-critical case**. We will mathematically treat the first two cases I/II.

3.4 Existence for the geometrically exact elastic micromorphic model

The following results extend the existence theorems for geometrically exact micromorphic micro-incompressible elastic solids given previously.[15]

Theorem 3.1 (Existence for elastic micromorphic model: case I.)
Let $\Omega \subset \mathbb{R}^3$ be a bounded Lipschitz domain and assume for the boundary data $g_{\mathrm{d}} \in H^1(\Omega, \mathbb{R}^3)$ and $P_{\mathrm{d}} \in W^{1,1+p}(\Omega, \mathrm{GL}^+(3, \mathbb{R}))$. Moreover, let the applied external potentials satisfy (3.6). *Then* (3.1) *with material constants conforming to case I and $p > 1$ admits at least one minimizing solution triple $(\varphi, \overline{P}, \overline{\alpha}_p) \in H^1(\Omega, \mathbb{R}^3) \times W^{1,1+p}(\Omega, \mathrm{SL}(3, \mathbb{R})) \times W^{1,2+p}(\Omega, \mathbb{R})$.*

Proof. We apply the direct methods of variations. The influence of the external potentials is gathered in writing $\Pi(\varphi, P)$. With the prescription of $(g_{\mathrm{d}}, P_{\mathrm{d}})$ it is clear that $I < \infty$ for exactly this pair of functions after decomposing P_{d} in its rotational, isochoric stretch and volumetric stretch. Since (3.6) is assumed, it is also clear that I is bounded below for all $\varphi \in L^1(\Omega, \mathbb{R}^3)$ and $P \in L^1(\Omega, \mathrm{GL}^+(3, \mathbb{R}))$.

We may therefore choose decreasing (infimizing) sequences of triples

$$(\varphi^k, \overline{P}^k, \overline{\alpha}_p^k) \in H^1(\Omega, \mathbb{R}^3) \times W^{1,1+p}(\Omega, \mathrm{SL}(3, \mathbb{R})) \times W^{1,2+p}(\Omega, \mathbb{R}), \tag{3.8}$$

such that

$$\lim_{k \to \infty} I(\varphi^k, \overline{P}^k, \overline{\alpha}_p^k) = \inf_{\substack{\varphi \in L^1(\Omega, \mathbb{R}^3), \\ \overline{P} \in L^1(\Omega, \mathrm{SL}(3, \mathbb{R})), \\ \overline{\alpha}_p \in L^1(\Omega, \mathbb{R})}} I(\varphi, \overline{P}, \overline{\alpha}_p). \tag{3.9}$$

The total curvature contribution W_{curv} along this sequence is bounded independent of the number k again on account of (3.6).[16]

Observe now that the micromorphic curvature term $\mathfrak{K}_p$ controls $\overline{P} \in W^{1,1+p}(\Omega, \mathrm{SL}(3, \mathbb{R}))$, since $\|\mathfrak{K}_p\| = \|\overline{R}_p^T \mathrm{D_x} \overline{P}\| = \|\mathrm{D_x} \overline{P}\|$, pointwise, the assumption that $\alpha_5, \alpha_6 > 0$ and the application of Poincarés inequality with the Dirichlet conditions on $\overline{P}$. Moreover, since $\alpha_8 > 0$ we

priori to verify an **unqualified coercivity condition** [65] of the type $W(F) \geq c^+ \|F\|^q - C$, $q > 1$, which, together with Dirichlet conditions and Poincaré's inequality controls the $L^q(\Omega)$ part of the deformation.

Fields satisfying (3.6) are e.g. the gravity field of a finite mass, the electric field of a finite charge etc. Remark as well that (3.6) does not exclude local, integrable singularities. The traditional dead load case in (3.5) must rather be interpreted as a linearization of the finite external potential: write $\varphi(x) = x + u(x)$, then $\Pi(x, \varphi(x)) = \Pi(x, x + u(x)) = \Pi(x, x) + \langle D_\varphi \Pi(x, x), u\rangle + \ldots = \mathrm{const.} + \langle f, u\rangle + \ldots$ with $f(x) = D_\varphi \Pi(x, x)$. We are not aware of a previous introduction of a condition similar to (3.6).

[15] The proposed finite results determine the macroscopic deformation $\varphi \in H^1(\Omega, \mathbb{R}^3)$ and nothing more. This means that discontinuous macroscopic deformations by cavities or the formation of holes are not excluded (possible mode I failure). If $\mu_c > 0$, fracture is effectively ruled out, which is unrealistic.

[16] If (3.6) does not hold, one might have infimizing sequences with unbounded curvature. The geometrically exact micromorphic formulation is only **conditionally coercive**.

obtain boundedness of $\overline{\alpha}_p^k \in W^{1,2+p}(\Omega,\mathbb{R})$, again independent of $k \in \mathbb{N}$. This result remains true already without specification of Dirichlet boundary conditions for $\overline{\alpha}_p$ since the term $e^{\overline{\alpha}_p}$ estimates any L^q-norm of $\overline{\alpha}_p$. For $p > 1$ Sobolev's embedding shows that we can choose a subsequence, not relabelled, such that strongly

$$\overline{\alpha}_p^k \to \widehat{\overline{\alpha}}_p \in C^0(\Omega,\mathbb{R}) \quad k \to \infty\,. \tag{3.10}$$

Now we may extract a subsequence again denoted by $\overline{P}^k$ converging strongly in $L^{1+p}(\Omega)$ to an element $\widehat{P} \in W^{1,1+p}(\Omega,\mathbb{M}^{3\times 3})$ since $p > 0$ by assumption. Moreover, a further subsequence can be found, such that the curvature tensor $\mathfrak{K}_{p,k}$ converges weakly to some $\widehat{\mathfrak{K}_p}$ in $L^{1+p}(\Omega)$. For $1 < (1+p) < 3$ the embedding

$$W^{1,1+p}(\Omega) \subset L^{\frac{3(1+p)}{3-(1+p)}-\delta}(\Omega)\,, \quad \delta \geq 0\,, \tag{3.11}$$

for three space dimensions is compact for $\delta > 0$ and shows that the subsequence $\overline{P}^k$ can be chosen such that it converges indeed strongly in the topology of $L^{6-\delta}(\Omega)$, since we have moreover $p \geq 1$, which implies immediately that $\widehat{P} \in W^{1,1+p}(\Omega,\mathrm{SL}(3,\mathbb{R}))$. If $1+p \geq 3$ we can use better embeddings to have the same conclusion.

Because $\mu_c > 0$, we have the simple algebraic estimate

$$\begin{aligned} W_{\mathrm{mp}}(P^{-1,k}F^k) &\geq \mu_c\,\|P^{-1,k}F^k - 1\!\!1\|^2 = \mu_c\,\left(\|P^{-1,k}F^k\|^2 - 2\langle P^{-1,k}F^k, 1\!\!1\rangle + 3\right) \\ &\geq \mu_c\left(\|\overline{U}_k\|^2 - 2\sqrt{3}\|\overline{U}_k\| + 3\right)\,, \end{aligned} \tag{3.12}$$

implying the boundedness of the micromorphic stretch $\overline{U}_k = P^{-1,k}F^k$ in $L^2(\Omega)$. Moreover, by Hölder's inequality, we obtain

$$\begin{aligned} \|F^k\|_{s,\Omega} &= \|P^kP^{-1,k}F^k\|_{s,\Omega} \leq \|P^k\|_{r_1,\Omega}\,\|P^{-1,k}F^k\|_{r_2,\Omega}\,, \quad \frac{1}{s} = \frac{1}{r_1} + \frac{1}{r_2}\,, \\ &= \|e^{\frac{\overline{\alpha}_p^k}{3}}\,\overline{P}^k\|_{r_1,\Omega}\,\|P^{-1,k}F^k\|_{r_2,\Omega}\,, \\ &\leq \sup_{x\in\Omega} e^{\frac{\overline{\alpha}_p^k(x)}{3}}\,\|\overline{P}^k\|_{r_1,\Omega}\,\|P^{-1,k}F^k\|_{r_2,\Omega}\,. \end{aligned} \tag{3.13}$$

Since $\overline{P}^k$ is bounded in $L^6(\Omega)$ (3.11) and $P^{-1,k}F^k$ is bounded in $L^2(\Omega)$ and $\overline{\alpha}_p^k$ is strongly converging in $C^0(\Omega,\mathbb{R})$ (3.10), we may choose $r_1 = 6$, $r_2 = 2$ to obtain boundedness of $F^k = \nabla\varphi_k$ in $L^s(\Omega)$, $s = \frac{3}{2}$. Using the Dirichlet boundary conditions for φ_k and the generalized Poincaré inequality we get

$$\|\varphi_k\|_{W^{1,s}(\Omega,\mathbb{R}^3)} \leq Const. \tag{3.14}$$

By the boundedness of φ^k in $W^{1,s}(\Omega,\mathbb{R}^3)$ we may extract a subsequence, not relabelled, such that $\varphi^k \rightharpoonup \hat{\varphi} \in W^{1,s}(\Omega,\mathbb{R}^3)$. Furthermore, we may always obtain a subsequence of (φ^k, P^k) such that $\overline{U}_k = P^{-1,k}F^k$ converges weakly in $L^2(\Omega)$ to some element $\widehat{\overline{U}}$ on account of the boundedness of the stretch energy and $\mu_c > 0$.

We have already shown that for $p \geq 1$ the sequence $\overline{P}^k$ converges indeed strongly in $L^r(\Omega)$ to an element $\widehat{\overline{P}} \in W^{1,1+p}(\Omega,\mathrm{SL}(3,\mathbb{R}))$. Therefore

$$\begin{aligned} \overline{P}^{-1,k} &= \frac{1}{\det[\overline{P}^k]}\,\mathrm{Adj}\,\overline{P}^k \to \frac{1}{\det[\widehat{\overline{P}}]}\,\mathrm{Adj}\,\widehat{\overline{P}} = \widehat{\overline{P}}^{-1} \;\text{in}\, L^{\frac{r}{2}}(\Omega,\mathrm{SL}(3,\mathbb{R}))\,, \\ r &= \frac{3(1+p)}{(3-(1+p))} - \delta\,, \quad \text{if}\ 1 < (1+p) < 3\,, \end{aligned} \tag{3.15}$$

and we obtain for $p > 1$ that $\overline{P}^{-1,k} \to \widehat{\overline{P}}^{-1}$ strong in $L^{3+\tilde{\delta}}(\Omega,\mathrm{SL}(3,\mathbb{R}))$, $\tilde{\delta} > 0$. Moreover,

$$P^{-1,k} = e^{-\frac{\overline{\alpha}_p^k}{3}}\,\overline{P}^{-1,k} \to \widehat{P}^{-1} = e^{-\frac{\widehat{\overline{\alpha}}_p}{3}}\,\widehat{\overline{P}}^{-1,k}\,, \tag{3.16}$$

on account of the strong convergence of $\overline{\alpha}_p^k$. Thus $\overline{P}^{-1,k}F^k$ converges certainly weakly to $\widehat{P}^{-1}F$ in $L^1(\Omega)$ on account of Hölder's inequality (sharp). The weak limit in $L^1(\Omega)$ must coincide with the weak limit of $\overline{U}_k$ in $L^2(\Omega)$. Hence the identity $\widehat{\overline{U}} = \widehat{P}^{-1}\nabla\hat{\varphi}$ holds.

Since the mapping polar : $\mathrm{GL}^+(3,\mathbb{R}) \mapsto \mathrm{SO}(3,\mathbb{R})$ is a bounded continuous function on invertible matrices with positive determinant, it generates a nonlinear superposition operator

$$\mathrm{polar}(\cdot) : L^r(\Omega, \mathrm{GL}^+(3,\mathbb{R})) \mapsto L^r(\Omega, \mathrm{SO}(3,\mathbb{R}))\,, \tag{3.17}$$

which, moreover, is continuous [3, p.101,Th.3.7]. Thus $\overline{R}_k = \mathrm{polar}(\overline{P}_k) \to \widehat{\overline{R}} = \mathrm{polar}(\widehat{\overline{P}})$ strongly in $L^r(\Omega)$ and a similar argument as for the sequence $\overline{U}_k$ shows that

$$\mathfrak{K}_{p,k} \rightharpoonup \widehat{\mathfrak{K}_p} = \mathrm{polar}(\widehat{P})^T \mathrm{D_x} \widehat{P}\,, \tag{3.18}$$

in $L^{1+p}(\Omega)$, weakly. Again on account of $\overline{P}^k \to \widehat{\overline{P}}$ in $L^r(\Omega, \mathrm{SL}(3,\mathbb{R}))$ we infer now

$$\overline{U}_p^k = \sqrt{\overline{P}^{k,T}\overline{P}^k} \to \sqrt{\widehat{\overline{P}}^T \widehat{\overline{P}}} = \widehat{\overline{U}}_p \quad \text{in } L^r(\Omega, \mathrm{SL}(3,\mathbb{R}))\,, \tag{3.19}$$

because the map $\mathbb{M}^{3\times 3} \mapsto \mathrm{PSym}(3)$, $X \mapsto \sqrt{X^T X}$ is continuous and has linear growth.

Since the total energy is convex in $(\overline{U}, \overline{U}_p, \mathfrak{K}_p, \nabla \overline{\alpha}_p)$ and continuous w.r.t. $\overline{\alpha}_p$, and the external potential Π is continuous w.r.t. strong convergence in $L^1(\Omega)$ on account of (3.6), we get

$$\begin{aligned}
I(\hat{\varphi}, \widehat{\overline{P}}, \widehat{\overline{\alpha}}_p) &= \int_\Omega W_{\mathrm{mp}}(\widehat{\overline{U}}) + W_{\mathrm{foam}}(\widehat{\overline{U}}_p, \widehat{\overline{\alpha}}_p) + W_{\mathrm{curv}}(\widehat{\mathfrak{K}_p}, \nabla \widehat{\overline{\alpha}}_p)\,\mathrm{dV} - \Pi(\hat{\varphi}, \widehat{P}) \\
&\le \liminf_{k\to\infty} \int_\Omega W_{\mathrm{mp}}(\overline{U}_k) + W_{\mathrm{foam}}(\overline{U}_p^k) + W_{\mathrm{curv}}(\mathfrak{K}_{p,k}, \nabla \overline{\alpha}_p^k)\,\mathrm{dV} - \Pi(\varphi_k, P_k) \\
&= \lim_{k\to\infty} I(\varphi^k, \overline{P}^k, \overline{\alpha}_p^k) = \inf_{\substack{\varphi \in L^1(\Omega,\mathbb{R}^3),\\ \overline{P} \in L^1(\Omega, \mathrm{SL}(3,\mathbb{R})),\\ \overline{\alpha}_p \in L^1(\Omega,\mathbb{R})}} I(\varphi, \overline{P}, \overline{\alpha}_p)\,,
\end{aligned} \tag{3.20}$$

which implies that the limit triple $(\hat{\varphi}, \widehat{P}, \widehat{\overline{\alpha}}_p)$ is a minimizer. Note that the limit microdeformations $P = e^{\frac{\overline{\alpha}_p}{3}} \overline{R}_p \overline{U}_p$ may fail to be continuous, if $p \le 2$ (non-existence or limit case of Sobolev embedding). Moreover, uniqueness cannot be ascertained, since $\mathrm{SL}(3,\mathbb{R})$ is a nonlinear manifold (and the considered problem is indeed highly nonlinear), such that convex combinations in $\mathrm{SL}(3,\mathbb{R})$ may leave $\mathrm{SL}(3,\mathbb{R})$. Since the functional I is differentiable, the minimizing pair is a stationary point and therefore a solution of the field equations (2.18). Note again that **the limit microdeformations may fail to be continuously distributed in space**. That under these unfavourable circumstances a minimizing solution may nevertheless be found is entirely due to $\mu_c > 0$ and $p > 1$. The proof simplifies considerably in the geometrically exact Cosserat micropolar case $\overline{P} \in \mathrm{SO}(3,\mathbb{R})$, in which case $p \ge 1$ is already sufficient. ■

We continue with the **super-critical** case which is more appropriate for macroscopic situations and closer to classical elasticity.

Theorem 3.2 (Existence for elastic micromorphic model: case II.)
Let $\Omega \subset \mathbb{R}^3$ be a bounded Lipschitz domain and assume for the boundary data $g_{\mathrm{d}} \in H^1(\Omega, \mathbb{R}^3)$ and $P_{\mathrm{d}} \in W^{1,1+p+q}(\Omega, \mathrm{SL}(3,\mathbb{R}))$. Moreover, let the applied external potentials satisfy (3.6). *Then* (3.1) *with material constants conforming to case II admits at least one minimizing solution triple $(\varphi, \overline{P}, \overline{\alpha}_p) \in H^1(\Omega,\mathbb{R}^3) \times W^{1,1+p+q}(\Omega, \mathrm{SL}(3,\mathbb{R})) \times W^{1,2+p}(\Omega,\mathbb{R})$.*

Proof. We repeat the arguments of case I. However, the boundedness of infimizing sequences is not immediately clear. Boundedness of the microdeformations $\overline{P}^k$ holds true in the space $W^{1,1+p+q}(\Omega, \mathrm{SL}(3,\mathbb{R}))$ with $1+p+q > N = 3$, hence we may extract a subsequence, not relabelled, such that $\overline{P}^k$ converges strongly to $\widehat{\overline{P}} \in C^0(\overline{\Omega}, \mathrm{SL}(3,\mathbb{R}))$ in the topology of $C^0(\overline{\Omega}, \mathrm{SL}(3,\mathbb{R}))$ on account of the Sobolev-embedding theorem. Since $P^{-1,k} = e^{-\frac{\overline{\alpha}_p^k}{3}} \overline{P}^{-1,k}$, we obtain as well that

$$P^{-1,k} \to \widehat{P}^{-1} \in C^0(\overline{\Omega}, \mathrm{GL}^+(3,\mathbb{R}))\,, \tag{3.21}$$

on account of strong convergence of $\overline{\alpha}_p^k$.

Along such strongly convergent sequence of microdeformations, the sequence of deformations φ^k is also bounded in $H^1(\Omega,\mathbb{R}^3)$. However, this is not due to a basically simple estimate as in case I, but only true after integration over the domain: at face value we only control certain mixed symmetric expressions in the deformation gradient. Let us define $u_k \in H^{1,2}(\omega, \mathbb{R}^3)$ by $\varphi^k = g_{\mathrm{d}} + (\varphi^k - g_{\mathrm{d}}) = g_{\mathrm{d}} + u_k$. Then we have

$$
\begin{aligned}
\infty > & I(g_{\mathrm{d}}, \overline{P}_{\mathrm{d}}, \overline{\alpha}_{p_{\mathrm{d}}}) > \int_\Omega W_{\mathrm{mp}}(\overline{U}_k) + W_{\mathrm{foam}}(\overline{U}_p^k, \overline{\alpha}_p^k) + W_{\mathrm{curv}}(\mathfrak{K}_{p,k}, \nabla \overline{\alpha}_p^k)\,\mathrm{dV} - \Pi(\varphi_k, P^k) \\
&\geq \int_\Omega W_{\mathrm{mp}}(\overline{U}_k)\,\mathrm{dV} - \Pi(\varphi_k, P^k) \geq \int_\Omega W_{\mathrm{mp}}(\overline{U}_k)\,\mathrm{dV} - C \\
&\geq \int_\Omega \frac{\mu_e}{4} \|P^{-1,k}\nabla\varphi_k + \nabla\varphi_k^T P^{-T,k} - 2\mathbb{1}\|^2\,\mathrm{dV} - C \qquad (3.22) \\
&= \int_\Omega \frac{\mu_e}{4} \|P^{-1,k}(\nabla u_k + \nabla g_{\mathrm{d}}) + (\nabla u_k + \nabla g_{\mathrm{d}})^T P^{-T,k} - 2\mathbb{1}\|^2\,\mathrm{dV} - C \\
&= \int_\Omega \frac{\mu_e}{4} \|P^{-1,k}\nabla u_k + \nabla u_k^T P^{-T,k}\|^2 \\
&\quad + \frac{2\mu_e}{4} \langle P^{-1,k}\nabla u_k + \nabla u_k^T P^{-T,k}, P^{-1,k}\nabla g_{\mathrm{d}} + \nabla g_{\mathrm{d}}^T P^{-T,k} - 2\mathbb{1}\rangle \\
&\quad + \frac{\mu_e}{4} \|P^{-1,k}\nabla g_{\mathrm{d}} + \nabla g_{\mathrm{d}}^T P^{-T,k} - 2\mathbb{1}\|^2\,\mathrm{dV} - C \\
&\geq \int_\Omega \frac{\mu_e}{4} \|P^{-1,k}\nabla u_k + \nabla u_k^T P^{-T,k}\|^2 \\
&\quad - \frac{\mu_e}{4} \left(\varepsilon\, \|P^{-1,k}\nabla u_k + \nabla u_k^T P^{-T,k}\|^2 + \frac{1}{\varepsilon} \|P^{-1,k}\nabla g_{\mathrm{d}} + \nabla g_{\mathrm{d}}^T P^{-T,k} - 2\mathbb{1}\|^2 \right) \\
&\quad + \frac{\mu_e}{4} \|P^{-1,k}\nabla g_{\mathrm{d}} + \nabla g_{\mathrm{d}}^T P^{-T,k} - 2\mathbb{1}\|^2\,\mathrm{dV} - C \\
&\geq \int_\Omega \frac{\mu_e}{8} \|P^{-1,k}\nabla u_k + \nabla u_k^T P^{-T,k}\|^2 \\
&\quad - \frac{\mu_e}{2} \|P^{-1,k}\nabla g_{\mathrm{d}} + \nabla g_{\mathrm{d}}^T P^{-T,k} - 2\mathbb{1}\|^2 \\
&\quad + \frac{\mu_e}{4} \|P^{-1,k}\nabla g_{\mathrm{d}} + \nabla g_{\mathrm{d}}^T P^{-T,k} - 2\mathbb{1}\|^2\,\mathrm{dV} - C \\
&= \int_\Omega \frac{\mu_e}{8} \|P^{-1,k}\nabla u_k + \nabla u_k^T P^{-T,k}\|^2 - \frac{\mu_e}{4} \|P^{-1,k}\nabla g_{\mathrm{d}} + \nabla g_{\mathrm{d}}^T P^{-T,k} - 2\mathbb{1}\|^2\,\mathrm{dV} - C \\
&\geq \int_\Omega \frac{\mu_e}{8} \|P^{-1,k}\nabla u_k + \nabla u_k^T P^{-T,k}\|^2\,\mathrm{dV} - C \\
&= \int_\Omega \frac{\mu_e}{8}\, \|(P^{-1,k} - \widehat{P}^{-1} + \widehat{P}^{-1})\nabla u_k + \nabla u_k^T (P^{-1,k} - \widehat{P}^{-1} + P^{-1})^T\|^2\,\mathrm{dV} - C \\
&\geq \int_\Omega \frac{\mu_e}{8} \underbrace{\|\widehat{P}^{-1}\nabla u_k + \nabla u_k^T \widehat{P}^{-T}\|^2}_{\text{combinations of derivatives}}\,\mathrm{dV} - C_2\, \|\widehat{P}^{-1} - P^{-1,k}\|_\infty\, \|u_k\|^2_{H^{1,2}(\Omega)} - C \\
&\geq \left(\frac{\mu_e}{8}\, c_K - C_2\, \|\widehat{P}^{-1} - P^{-1,k}\|_\infty\right) \|u_k\|^2_{H^{1,2}(\Omega)} - C\,,
\end{aligned}
$$

where we used Young's inequality with $\varepsilon = \frac{1}{2}$, made use of the appropriate Dirichlet boundary conditions for u_k and applied the extended Korn's inequality (7.1) in the improved version of [66] yielding the positive constant c_K for the **continuous** microdeformation $\widehat{P}^{-1}$. Since $\|\widehat{P}^{-1} - P^{-1,k}\|_\infty \to 0$ for $k \to \infty$ due to (3.21) we are able to conclude the boundedness of u_k in $H^1(\Omega)$. Hence, φ_k is bounded in $H^1(\Omega)$. Now we obtain that $\overline{U_k} \rightharpoonup \widehat{\overline{U}} = \widehat{P}^{-1}\nabla\hat{\varphi}$ by construction with the notations as in case I. The remainder proceeds as in case I. This finishes the argument. The limit microdeformations $\widehat{P}$ are indeed found to be continuous. ■

4 The infinitesimal micromorphic elastic solid

4.1 The variational formulation

Starting from the proposed finite-strain formulation and not intrinsically linear (as below in section 4.5), we may obtain a linear, infinitesimal micromorphic model by expanding all appearing variables to first order and keeping only quadratic terms in the energy expression.

Thus we write $F = 1\!\!1 + \nabla u$, $P = 1\!\!1 + p$, and the model turns into the problem of finding a pair $(u,p) : \Omega \subset \mathbb{R}^3 \mapsto \mathbb{R}^3 \times \mathfrak{gl}^+(3,\mathbb{R})$ of macroscopic displacement u and **independent, infinitesimal microdeformation** p satisfying

$$
\begin{aligned}
&\int_\Omega W_{\mathrm{mp}}(\overline{\varepsilon}, p) + W_{\mathrm{curv}}(\mathfrak{k}_p, \nabla \mathrm{tr}\,[p])\,\mathrm{dV} \mapsto \min . \text{ w.r.t. } (u,p),\\
&\qquad \overline{\varepsilon} = \nabla u - p, \quad p_{|_\Gamma} = p_{\mathrm{d}} \in \mathfrak{gl}^+(3,\mathbb{R}) = \mathbb{M}^{3\times 3}, \quad \varphi_{|_\Gamma} = g_{\mathrm{d}}\,, \qquad (4.1)\\
&W_{\mathrm{mp}}(\overline{\varepsilon}, p) = \mu_e \,\|\mathrm{sym}\,\overline{\varepsilon}\|^2 + \mu_c\,\|\mathrm{skew}\,\overline{\varepsilon}\|^2 + \frac{\lambda_e}{2}\,\mathrm{tr}\,[\mathrm{sym}\,\overline{\varepsilon}]^2 + \mu^{\mathrm{m}}\,\|\mathrm{sym}\,p\|^2 + \frac{\lambda^{\mathrm{m}}}{2}\mathrm{tr}\,[\mathrm{sym}\,p]^2\\
&\qquad = \mu_e\,\|\mathrm{sym}\,\nabla u - \mathrm{sym}\,p\|^2 + \mu_c\,\|\mathrm{skew}(\nabla u - p)\|^2 + \frac{\lambda_e}{2}\,\mathrm{tr}\,[\nabla u - p]^2\\
&\qquad + \mu^{\mathrm{m}}\,\|\mathrm{sym}\,p\|^2 + \frac{\lambda^{\mathrm{m}}}{2}\mathrm{tr}\,[p]^2\,,\\
&W_{\mathrm{curv}}(\mathfrak{k}_p, \nabla \mathrm{tr}\,[p]) = \mu \frac{L_c^2}{12}\left(\alpha_5\,\|\mathrm{sym}\,\mathfrak{k}_p\|^2 + \alpha_6\,\|\mathrm{skew}\,\mathfrak{k}_p\|^2 + \alpha_7\,\mathrm{tr}\,[\mathfrak{k}_p]^2 + \alpha_8\,\|\nabla \mathrm{tr}\,[p]\|^2\right)\,,\\
&\qquad \mathfrak{k}_p = \mathrm{D_x}[\mathrm{dev}\,p] = (\nabla(\mathrm{dev}\,p.e_1), \nabla(\mathrm{dev}\,p.e_2), \nabla(\mathrm{dev}\,p.e_3))\;.
\end{aligned}
$$

Here, $\mathfrak{k}_p$ is the third order infinitesimal curvature tensor, defined only on the purely distortional part of the infinitesimal microdeformation $\mathrm{dev}\,p$. If $\mu_e, \mu^{\mathrm{m}} > 0$ and $\mu_c, \lambda_e, \lambda^{\mathrm{m}} \geq 0$ it is an easy matter to show existence and uniqueness. For $\mu_c = 0$ we have to invoke the classical Korn's first inequality. It should be observed that even if $\mu_c = 0$ there remains a coupling of the two fields (u,p) due to the remaining coupling in the symmetric terms.

4.2 The linear system of balance equations

The linearized macroscopic force balance equation is obtained by taking free variations with respect to the total displacement u. Hence we obtain

$$
\mathrm{Div}\,\sigma(\nabla u, p) = 0, \quad u_{|_\Gamma}(x) = g_{\mathrm{d}}(x) - x\,, \qquad (4.2)
$$

with

$$
\sigma(\nabla u, p) = 2\mu_e\;(\mathrm{sym}\,\nabla u - \mathrm{sym}\,p) + 2\mu_c\;(\mathrm{skew}\,\nabla u - \mathrm{skew}\,p) + \lambda_e\,\mathrm{tr}\,[\nabla u - p]\cdot 1\!\!1\,. \qquad (4.3)
$$

The remaining system of nine balance equations for the nine additional components of $p \in \mathfrak{gl}^+(3,\mathbb{R}) = \mathbb{M}^{3\times 3}$ is obtained by taking free variations with respect to p which results in

$$
\begin{aligned}
\mathrm{dev}\,\mathrm{Div}\,D_{\mathfrak{k}_p} W_{\mathrm{curv}}(\mathfrak{k}_p, \nabla \mathrm{tr}\,[p]) &= \mathrm{dev}\,(-2\mu_e\;(\mathrm{sym}\,\nabla u - \mathrm{sym}\,p)\\
&\quad - 2\mu_c\;(\mathrm{skew}\,\nabla u - \mathrm{skew}\,p) - \lambda_e\,\mathrm{tr}\,[\nabla u - p]\,1\!\!1\\
&\quad + 2\mu^{\mathrm{m}}\;\mathrm{sym}\,p + \lambda^{\mathrm{m}}\,\mathrm{tr}\,[p]\cdot 1\!\!1)\;,\\
\mathrm{Div}\,D_{\nabla \mathrm{tr}[p]} W_{\mathrm{curv}}(\mathfrak{k}_p, \nabla \mathrm{tr}\,[p]) &= \mathrm{tr}\,(-2\mu_e\;(\mathrm{sym}\,\nabla u - \mathrm{sym}\,p)\\
&\quad - 2\mu_c\;(\mathrm{skew}\,\nabla u - \mathrm{skew}\,p) - \lambda_e\,\mathrm{tr}\,[\nabla u - p]\,1\!\!1\\
&\quad + 2\mu^{\mathrm{m}}\;\mathrm{sym}\,p + \lambda^{\mathrm{m}}\,\mathrm{tr}\,[p]\cdot 1\!\!1)\;. \qquad (4.4)
\end{aligned}
$$

This is equivalent to

$$
\begin{aligned}
0 &= \mathrm{dev}\,\sigma(\nabla u, p) - 2\mu^{\mathrm{m}}\;\mathrm{dev}\,\mathrm{sym}\,p + \mathrm{dev}\,\mathrm{Div}\,D_{\mathfrak{k}_p} W_{\mathrm{curv}}(\mathfrak{k}_p, \nabla \mathrm{tr}\,[p])\,,\\
0 &= \mathrm{tr}\,[\sigma(\nabla u, p)] - (2\mu^{\mathrm{m}} + 3\lambda^{\mathrm{m}})\,\mathrm{tr}\,[p] + \mathrm{Div}\,D_{\nabla \mathrm{tr}[p]} W_{\mathrm{curv}}(\mathfrak{k}_p, \nabla \mathrm{tr}\,[p])\,. \qquad (4.5)
\end{aligned}
$$

4.3 Calculation of consistent effective elastic moduli

It is of prime importance to have values of μ_e, λ_e at hand which are consistent with the classical linear elastic model for long wave-length (large samples). Considering very large samples of the cellular structure amounts to letting $L_c \geq 0$, the characteristic length, tend to zero. As a consequence of $L_c = 0$ the two equations (4.5) loose the curvature terms and turn into

$$
\begin{aligned}
0 &= \mathrm{dev}\,\sigma(\nabla u, p) - 2\mu^{\mathrm{m}}\;\mathrm{dev}\,\mathrm{sym}\,p\,, \qquad (4.6)\\
0 &= \mathrm{tr}\,[\sigma(\nabla u, p)] - (2\mu^{\mathrm{m}} + 3\lambda^{\mathrm{m}})\,\mathrm{tr}\,[p]\,,
\end{aligned}
$$

expressing an algebraic side-condition. Inserting formula (4.3) for σ into (4.6) allows us to obtain after some lengthy but straightforward computations the following algebraic relations

$$\begin{aligned} \operatorname{tr}[p] &= \frac{(2\mu_e + 3\lambda_e)}{2(\mu_e + \mu^{\mathrm{m}}) + 3(\lambda_e + \lambda^{\mathrm{m}})} \operatorname{tr}[\nabla u]\,, \\ \operatorname{dev}\operatorname{sym} p &= \frac{\mu_e}{(\mu_e + \mu^{\mathrm{m}})} \operatorname{dev}\operatorname{sym}\nabla u\,, \\ \operatorname{dev}\operatorname{skew} p &= \operatorname{dev}\operatorname{skew}\nabla u\,, \qquad (\mu_c \text{ not involved!})\,, \end{aligned} \tag{4.7}$$

where we used that the operator dev is orthogonal to $\mathbb{R}\cdot 1\!\!1$ and sym is orthogonal to skew and $\operatorname{dev}\operatorname{skew} = \operatorname{skew}$. Moreover,

$$\begin{aligned} \operatorname{tr}[\nabla u - p] &= \left(1 - \frac{(2\mu_e + 3\lambda_e)}{2(\mu_e + \mu^{\mathrm{m}}) + 3(\lambda_e + \lambda^{\mathrm{m}})}\right) \operatorname{tr}[\nabla u] \\ &= \frac{(2\mu^{\mathrm{m}} + 3\lambda^{\mathrm{m}})}{(2\mu^{\mathrm{m}} + 3\lambda^{\mathrm{m}}) + (2\mu_e + 3\lambda_e)} \operatorname{tr}[\nabla u]\,. \end{aligned} \tag{4.8}$$

Reinserting the results into (4.3) yields, after taking dev on both sides

$$\begin{aligned} \operatorname{dev}\sigma(\nabla u, p) &= 2\mu_e\,(\operatorname{dev}\operatorname{sym}\nabla u - \operatorname{dev}\operatorname{sym} p) + 2\mu_c\,(\operatorname{skew}\nabla u - \operatorname{skew} p) \\ &= 2\mu_e\left(\operatorname{dev}\operatorname{sym}\nabla u - \frac{\mu_e}{(\mu_e + \mu^{\mathrm{m}})}\operatorname{dev}\operatorname{sym}\nabla u\right) + 2\mu_c\,(\operatorname{skew}\nabla u - 1\cdot\operatorname{skew}\nabla u) \\ &= 2\mu_e\left(1 - \frac{\mu_e}{(\mu_e + \mu^{\mathrm{m}})}\right)\operatorname{dev}\operatorname{sym}\nabla u = 2\mu_e\frac{\mu^{\mathrm{m}}}{(\mu_e + \mu^{\mathrm{m}})}\operatorname{dev}\operatorname{sym}\nabla u\,. \end{aligned} \tag{4.9}$$

Similarly, reinserting the results into (4.3) yields, after taking the trace on both sides

$$\begin{aligned} \operatorname{tr}[\sigma(\nabla u, p)] &= 2\mu_e \operatorname{tr}[\operatorname{sym}\nabla u - \operatorname{sym} p] + 2\mu_c \operatorname{tr}[\operatorname{skew}\nabla u - \operatorname{skew} p] + \lambda_e \operatorname{tr}[\nabla u - p]\cdot\operatorname{tr}[1\!\!1] \\ &= 2\mu_e \operatorname{tr}[\nabla u - p] + 3\lambda_e \operatorname{tr}[\nabla u - p] = (2\mu_e + 3\lambda_e)\,\operatorname{tr}[\nabla u - p] \\ &= (2\mu_e + 3\lambda_e)\,\frac{(2\mu^{\mathrm{m}} + 3\lambda^{\mathrm{m}})}{(2\mu^{\mathrm{m}} + 3\lambda^{\mathrm{m}}) + (2\mu_e + 3\lambda_e)}\operatorname{tr}[\nabla u]\,. \end{aligned} \tag{4.10}$$

For a linear elastic isotropic solid, which represents the macroscopic stress-strain relation for large samples, one has the classical relation

$$\begin{aligned} &\sigma = 2\mu\,\operatorname{sym}\nabla u + \lambda\operatorname{tr}[\nabla u]\cdot 1\!\!1 \quad \Rightarrow \\ &\operatorname{dev}\sigma = 2\mu\,\operatorname{dev}\operatorname{sym}\nabla u \quad \text{and} \quad \operatorname{tr}[\sigma] = (2\mu + 3\lambda)\,\operatorname{tr}[\nabla u]\,. \end{aligned} \tag{4.11}$$

Upon comparing coefficients of (4.11) with (4.9) and (4.10) we identify

$$\begin{aligned} 2\mu &= 2\mu_e\frac{\mu^{\mathrm{m}}}{(\mu_e + \mu^{\mathrm{m}})}\,, \\ (2\mu + 3\lambda) &= (2\mu_e + 3\lambda_e)\,\frac{(2\mu^{\mathrm{m}} + 3\lambda^{\mathrm{m}})}{(2\mu^{\mathrm{m}} + 3\lambda^{\mathrm{m}}) + (2\mu_e + 3\lambda_e)}\,. \end{aligned} \tag{4.12}$$

This implies that in our model the **large scale shear modulus** μ is half the **harmonic mean**[17] of the **relative elastic shear modulus** μ_e and the **microstructural shear modulus** μ^{m}, while the **large scale bulk modulus** $\kappa = \frac{2\mu+3\lambda}{3}$ is half the **harmonic mean** of the **relative elastic bulk modulus** κ_e and the **microstructural bulk modulus** κ^{m}.

Hence, solving in a first step for the **relative elastic shear modulus** μ_e and the **relative elastic bulk modulus** $\kappa_e = \frac{2\mu_e+3\lambda_e}{3}$, yields

$$\mu_e = \frac{\mu^{\mathrm{m}}\,\mu}{(\mu^{\mathrm{m}} - \mu)}\,, \quad 3\kappa_e = (2\mu_e + 3\lambda_e) = \frac{(2\mu + 3\lambda)\,(2\mu^{\mathrm{m}} + 3\lambda^{\mathrm{m}})}{(2\mu^{\mathrm{m}} + 3\lambda^{\mathrm{m}}) - (2\mu + 3\lambda)}\,. \tag{4.13}$$

Therefore

$$\mu_e = \frac{\mu^{\mathrm{m}}\,\mu}{(\mu^{\mathrm{m}} - \mu)}\,, \quad 3\lambda_e = \frac{(2\mu + 3\lambda)\,(2\mu^{\mathrm{m}} + 3\lambda^{\mathrm{m}})}{(2(\mu^{\mathrm{m}} - \mu) + 3(\lambda^{\mathrm{m}} - \lambda))} - 2\frac{\mu^{\mathrm{m}}\,\mu}{(\mu^{\mathrm{m}} - \mu)}\,. \tag{4.14}$$

[17] $\mathcal{H}(\alpha,\beta) = \frac{2}{\frac{1}{\alpha}+\frac{1}{\beta}} = \frac{2\alpha\beta}{\alpha+\beta}$ for $\alpha,\beta > 0$, compare with the **Reuss-bounds** in homogenization theory.

This result motivates that the "macroscopic" Lamé moduli μ, λ must always be smaller than the microscopic moduli $\mu^{\rm m}, \lambda^{\rm m}$ related to the response of a representative volume element (RVE) of the substructure. This is physically consistent: the large-scale sample cannot possibly be stiffer than the constitutive substructure. Let us consider the interesting limit cases in (4.12):

$$\begin{aligned}
\textbf{micro-incompressible:}\quad & \lambda^{\rm m} \to \infty\,, \quad \mu^{\rm m} < \infty \quad \Rightarrow \quad \lambda = \lambda_e + \frac{2\mu^2}{3(\mu^{\rm m}-\mu)}\,,\\
\textbf{microstretch:}\quad & \mu^{\rm m} \to \infty\,, \quad \lambda^{\rm m} < \infty \quad \Rightarrow \quad \lambda = \lambda_e\,, \quad \mu = \mu_e\,,\\
\textbf{micropolar:}\quad & \mu^{\rm m} \to \infty\,, \quad \lambda^{\rm m} \to \infty \quad \Rightarrow \quad \lambda = \lambda_e\,, \quad \mu = \mu_e\,.
\end{aligned} \tag{4.15}$$

4.4 Identification with Mindlin's representation

Many papers on linearized micromorphic models start from a representation of the free-energy function based on Mindlin's work [55, 5.5], e.g.[45]. A major drawback of Mindlin's representation is, however, that no account has been taken, to ensure overall positivity of the quadratic energy. This has to be checked additionally and can be quite labourous because of many appearing coefficients. We consider only the local part (the part without curvature) of Mindlin's representation. Let us define

$$\varepsilon = \operatorname{sym}\nabla u\,, \qquad \overline{\varepsilon} := \nabla u - p\,. \tag{4.16}$$

Then Mindlin's local energy contribution $W_{\rm mp}^{\rm Mind}$ with seven material constants $\widehat{\mu}, \widehat{\lambda}, b_1, b_2, b_3, g_1, g_2$ reads

$$\begin{aligned}
W_{\rm mp}^{\rm Mind}(\nabla u, p) = W_{\rm mp}^{\rm Mind}(\varepsilon, \overline{\varepsilon}) = \frac{\widehat{\lambda}}{2}\operatorname{tr}[\varepsilon]^2 + \widehat{\mu}\,\|\varepsilon\|^2 + \frac{b_1}{2}\operatorname{tr}[\overline{\varepsilon}]^2 + \frac{b_2}{2}\|\overline{\varepsilon}\|^2 + \frac{b_3}{2}\langle\overline{\varepsilon}, \overline{\varepsilon}^T\rangle&\\
+ g_1 \operatorname{tr}[\varepsilon]\operatorname{tr}[\overline{\varepsilon}] + 2\,g_2\,\langle\varepsilon, \overline{\varepsilon}\rangle\,.&
\end{aligned} \tag{4.17}$$

Note that this defines a quadratic form, whose positive-definiteness is not ensured by taking positive parameters $\widehat{\mu}, \widehat{\lambda}, \ldots$. In comparison, in (4.1) we have proposed a five material constants representation, which automatically defines a positive quadratic form, if the coefficients are positive themselves.[18] The proposed quadratic representation in (4.1) reads

$$\begin{aligned}
W_{\rm mp}(\overline{\varepsilon}, p) &= \mu_e\,\|\operatorname{sym}\overline{\varepsilon}\|^2 + \mu_c\,\|\operatorname{skew}\overline{\varepsilon}\|^2 + \frac{\lambda_e}{2}\operatorname{tr}[\operatorname{sym}\overline{\varepsilon}]^2 + \mu^{\rm m}\,\|\operatorname{sym}p\|^2 + \frac{\lambda^{\rm m}}{2}\operatorname{tr}[\operatorname{sym}p]^2\\
&= \mu_e\,\|\operatorname{sym}\overline{\varepsilon}\|^2 + \mu_c\,\|\operatorname{skew}\overline{\varepsilon}\|^2 + \frac{\lambda_e}{2}\operatorname{tr}[\operatorname{sym}\overline{\varepsilon}]^2 + \mu^{\rm m}\,\|\operatorname{sym}p - \varepsilon + \varepsilon\|^2\\
&\quad + \frac{\lambda^{\rm m}}{2}\operatorname{tr}[\operatorname{sym}p - \varepsilon + \varepsilon]^2\\
&= \mu_e\,\|\operatorname{sym}\overline{\varepsilon}\|^2 + \mu_c\,\|\operatorname{skew}\overline{\varepsilon}\|^2 + \frac{\lambda_e}{2}\operatorname{tr}[\operatorname{sym}\overline{\varepsilon}]^2\\
&\quad + \mu^{\rm m}\,\left(\|\operatorname{sym}p - \varepsilon\|^2 + 2\langle\operatorname{sym}p - \varepsilon, \varepsilon\rangle + \|\varepsilon\|^2\right)\\
&\quad + \frac{\lambda^{\rm m}}{2}\left(\operatorname{tr}[\operatorname{sym}p - \varepsilon]^2 + 2\operatorname{tr}[\operatorname{sym}p - \varepsilon]\operatorname{tr}[\varepsilon] + \operatorname{tr}[\varepsilon]^2\right)\\
&= (\mu_e + \mu^{\rm m})\,\|\operatorname{sym}\overline{\varepsilon}\|^2 + \mu_c\,\|\operatorname{skew}\overline{\varepsilon}\|^2 + \frac{(\lambda_e + \lambda^{\rm m})}{2}\operatorname{tr}[\operatorname{sym}\overline{\varepsilon}]^2\\
&\quad + \mu^{\rm m}\,\|\varepsilon\|^2 + \frac{\lambda^{\rm m}}{2}\operatorname{tr}[\varepsilon]^2\\
&\quad - 2\mu^{\rm m}\langle\varepsilon - \operatorname{sym}p, \varepsilon\rangle - \lambda^{\rm m}\operatorname{tr}[\varepsilon - \operatorname{sym}p]\operatorname{tr}[\varepsilon]\\
&= (\mu_e + \mu^{\rm m})\,\|\operatorname{sym}\overline{\varepsilon}\|^2 + \mu_c\,\|\operatorname{skew}\overline{\varepsilon}\|^2 + \frac{(\lambda_e + \lambda^{\rm m})}{2}\operatorname{tr}[\operatorname{sym}\overline{\varepsilon}]^2\\
&\quad + \mu^{\rm m}\,\|\varepsilon\|^2 + \frac{\lambda^{\rm m}}{2}\operatorname{tr}[\varepsilon]^2 - 2\mu^{\rm m}\langle\overline{\varepsilon}, \varepsilon\rangle - \lambda^{\rm m}\operatorname{tr}[\overline{\varepsilon}]\operatorname{tr}[\varepsilon]\\
&= (\mu_e + \mu^{\rm m})\,\|\frac{1}{2}(\overline{\varepsilon} + \overline{\varepsilon}^T)\|^2 + \mu_c\,\|\frac{1}{2}(\overline{\varepsilon} - \overline{\varepsilon}^T)\|^2 + \frac{(\lambda_e + \lambda^{\rm m})}{2}\operatorname{tr}[\operatorname{sym}\overline{\varepsilon}]^2\\
&\quad + \mu^{\rm m}\,\|\varepsilon\|^2 + \frac{\lambda^{\rm m}}{2}\operatorname{tr}[\varepsilon]^2 - 2\mu^{\rm m}\langle\overline{\varepsilon}, \varepsilon\rangle - \lambda^{\rm m}\operatorname{tr}[\overline{\varepsilon}]\operatorname{tr}[\varepsilon]
\end{aligned} \tag{4.18}$$

[18] This can be slightly weakened: $2\mu_e + 3\lambda_e \geq 0, 2\mu^{\rm m} + 3\lambda^{\rm m} \geq 0$, $\mu_e, \mu^{\rm m}, \mu_c \geq 0$ is sufficient.

$$
\begin{aligned}
&= \frac{(\mu_e+\mu^{\rm m})}{4}\,\|\overline{\varepsilon}+\overline{\varepsilon}^T\|^2 + \frac{\mu_c}{4}\,\|\overline{\varepsilon}-\overline{\varepsilon}^T\|^2 + \frac{(\lambda_e+\lambda^{\rm m})}{2}\,{\rm tr}\left[\overline{\varepsilon}\right]^2 \\
&\quad + \mu^{\rm m}\,\|\varepsilon\|^2 + \frac{\lambda^{\rm m}}{2}\,{\rm tr}\left[\varepsilon\right]^2 - 2\mu^{\rm m}\langle\overline{\varepsilon},\varepsilon\rangle - \lambda^{\rm m}\,{\rm tr}\left[\overline{\varepsilon}\right]{\rm tr}\left[\varepsilon\right] \\
&= \frac{(\mu_e+\mu^{\rm m})}{2}\,\left(\|\overline{\varepsilon}\|^2 + \langle\overline{\varepsilon},\overline{\varepsilon}^T\rangle\right) + \frac{\mu_c}{2}\,\left(\|\overline{\varepsilon}\|^2 - \langle\overline{\varepsilon},\overline{\varepsilon}^T\rangle\right) + \frac{(\lambda_e+\lambda^{\rm m})}{2}\,{\rm tr}\left[\overline{\varepsilon}\right]^2 \\
&\quad + \mu^{\rm m}\,\|\varepsilon\|^2 + \frac{\lambda^{\rm m}}{2}\,{\rm tr}\left[\varepsilon\right]^2 - 2\mu^{\rm m}\langle\overline{\varepsilon},\varepsilon\rangle - \lambda^{\rm m}\,{\rm tr}\left[\overline{\varepsilon}\right]{\rm tr}\left[\varepsilon\right] \\
&= \frac{(\mu_e+\mu^{\rm m}+\mu_c)}{2}\,\|\overline{\varepsilon}\|^2 + \frac{(\mu_e+\mu^{\rm m}-\mu_c)}{2}\langle\overline{\varepsilon},\overline{\varepsilon}^T\rangle + \frac{(\lambda_e+\lambda^{\rm m})}{2}\,{\rm tr}\left[\overline{\varepsilon}\right]^2 \\
&\quad + \mu^{\rm m}\,\|\varepsilon\|^2 + \frac{\lambda^{\rm m}}{2}\,{\rm tr}\left[\varepsilon\right]^2 - 2\mu^{\rm m}\langle\overline{\varepsilon},\varepsilon\rangle - \lambda^{\rm m}\,{\rm tr}\left[\overline{\varepsilon}\right]{\rm tr}\left[\varepsilon\right].
\end{aligned}
$$

Hence, comparing with Mindlin's representation (4.17) we are able to identify

$$
\begin{aligned}
&\widehat{\mu} = \mu^{\rm m}, \qquad \widehat{\lambda} = \lambda^{\rm m}, \qquad b_1 = \lambda_e + \lambda^{\rm m}\,, \\
&b_2 = \mu_e + \mu^{\rm m} + \mu_c, \qquad b_3 = \mu_e + \mu^{\rm m} - \mu_c\,, \\
&g_1 = -\lambda^{\rm m}, \qquad g_2 = -\mu^{\rm m}\,.
\end{aligned} \tag{4.19}
$$

Mindlin proposes [55, p.60]

$$
\begin{aligned}
&3b_1 + b_2 + b_3 \geq 0\,, \quad b_2 + b_3 \geq 0\,, \quad b_2 - b_3 \geq 0\,, \\
&(\Rightarrow \quad \kappa_e + \kappa^{\rm m} \geq 0\,, \quad \mu_e + \mu_m \geq 0\,, \quad \mu_c \geq 0)
\end{aligned} \tag{4.20}
$$

as **necessary conditions for a positive definite energy function** which is (of course) verified for (4.1).

Remark 4.1
It is not clear to us, whether Mindlin's seven parameter representation of the local strain-energy can be obtained by consistently linearizing a finite-strain micromorphic model.

4.5 The intrinsically linear micromorphic model

Several sets of generalized strain measures can be defined if one starts in an intrinsically linear context with no reference to some underlying finite-strain micromorphic model. The strain measures used in [35] are retained for the computational part of this work:

$$
\varepsilon = \frac{1}{2}(\nabla u + (\nabla u)^T), \quad \overline{\varepsilon} = \nabla u - p, \quad K = {\rm D_x} p\,, \tag{4.21}
$$

i.e. the **total strain** ε , the **relative deformation** $\overline{\varepsilon}$ and the third–rank **micro–deformation gradient tensor** K.[19]Three generalized stress tensors may be introduced in the virtual power of internal and contact forces:

$$
\pi^{(i)}(u,p) = \langle\sigma,\dot{\varepsilon}\rangle + \langle s,\dot{\overline{\varepsilon}}\rangle + \langle S,\dot{K}\rangle, \quad \pi^{(c)}(u,p) = \langle t,\dot{u}\rangle + \langle M,\dot{p}\rangle\,, \tag{4.22}
$$

where the second–rank stress tensor σ is symmetric but should not be confused with the classical Cauchy stress tensor. The additional stress tensors s and S respectively are second and third–rank tensors. The balance of momentum and balance of moment of momentum equations read, in the absence of volume forces or generalized couples (nor double forces):

$$
{\rm Div}(\sigma + s) = 0, \quad {\rm Div}\, S + s = 0\,. \tag{4.23}
$$

They are coupled thanks to the micro–stress tensor s. Equilibrium at the boundary reads

$$
t = (\sigma + s).\vec{n}, \quad M = S.\vec{n}\,, \tag{4.24}
$$

where the outer surface normal vector is denoted by $\vec{n}$.

[19]Note that we have given up the decoupling of the curvature into volumetric and distortional parts, contrary to (4.1).

In a linearized elastic micromorphic solid, the Helmholtz free energy is assumed to be a quadratic form $W^\sharp_{\rm lin}(\varepsilon, \overline{\varepsilon}, K)$ of the previous strain measures (4.21). The state laws are then deduced from the exploitation of the entropy principle of thermodynamics [33]:

$$\sigma = \rho \frac{\partial W^\sharp_{\rm lin}}{\partial \varepsilon}, \quad s = \rho \frac{\partial W^\sharp_{\rm lin}}{\partial \overline{\varepsilon}}, \quad S = \rho \frac{\partial W^\sharp_{\rm lin}}{\partial K} \tag{4.25}$$

The most general form of the potential for an isotropic linear elastic micromorphic medium has been proposed by Mindlin [55] based on such an intrinsically linear development. Keeping the original index notation for the proposed invariants of the strain tensors and the material moduli, it reads:

$$\begin{aligned} W^\sharp_{\rm lin} &= \frac{1}{2}\widehat{\lambda}\,\varepsilon_{ii}\varepsilon_{jj} + \widehat{\mu}\,\varepsilon_{ij}\varepsilon_{ij} + \frac{1}{2}b_1\,\overline{\varepsilon}_{ii}\overline{\varepsilon}_{jj} + \frac{1}{2}b_2\,\overline{\varepsilon}_{ij}\overline{\varepsilon}_{ij} + \frac{1}{2}b_3\,\overline{\varepsilon}_{ij}\overline{\varepsilon}_{ji} \\ &+ g_1\,\varepsilon_{ii}\overline{\varepsilon}_{jj} + g_2\,\varepsilon_{ij}(\overline{\varepsilon}_{ij} + \overline{\varepsilon}_{ji}) \\ &+ A_1K_{iik}K_{kkj} + A_2K_{iik}K_{jkj} + \frac{1}{2}A_3K_{iik}K_{jkk} + \frac{1}{2}A_4K_{ijj}K_{ikk} \\ &+ A_5K_{ijj}K_{kik} + \frac{1}{2}A_8K_{iji}K_{kjk} + \frac{1}{2}A_{10}K_{ijk}K_{ijk} \\ &+ A_{11}K_{ijk}K_{jki} + \frac{1}{2}A_{13}K_{ijk}K_{ikj} + \frac{1}{2}A_{14}K_{ijk}K_{jik} \\ &+ \frac{1}{2}A_{15}K_{ijk}K_{kji}\,, \end{aligned} \tag{4.26}$$

from which the constitutive relations

$$\begin{aligned} \sigma &= \widehat{\lambda}\,\mathrm{tr}\,[\varepsilon]\cdot 1\!\!1 + 2\widehat{\mu}\,\varepsilon + g_1\,\mathrm{tr}\,[\overline{\varepsilon}]\cdot 1\!\!1 + 2g_2\,\mathrm{sym}\,\overline{\varepsilon}\,, \\ s &= g_1\,\mathrm{tr}\,[\varepsilon]\cdot 1\!\!1 + 2g_2\,\varepsilon + b_1\,\mathrm{tr}\,[\overline{\varepsilon}]\cdot 1\!\!1 + b_2\,\overline{\varepsilon} + b_3\,\overline{\varepsilon}^T\,, \end{aligned} \tag{4.27}$$

and

$$\begin{aligned} S_{pqr} &= A_1(K_{rii}\delta_{pq} + K_{iip}\delta_{qr}) + A_2(K_{iiq}\delta_{pr} + K_{iri}\delta_{pq}) + A_3K_{jjr}\delta_{pq} \\ &+ A_4K_{pii}\delta_{qr} + A_5(K_{ipi}\delta_{qr} + K_{qii}\delta_{pr}) + A_8K_{iqi}\delta_{pr} \\ &+ A_{10}K_{pqr} + A_{11}(K_{qrp} + K_{rpq}) + A_{13}K_{prq} \\ &+ A_{14}K_{qpr} + A_{15}K_{rqp}\,, \end{aligned} \tag{4.28}$$

are deduced. Hence, the most general isotropic linear elastic relations involve $7 + 11 = 18$ constants. It should again be noted that the constants $\widehat{\mu}, \widehat{\lambda}$ cannot automatically be identified with the classical Lamé constants, despite appearance. The coefficients A_i have the dimension of a bending stiffness modulus: MPa.m^2.

In order to achieve positivity for the curvature part of the energy and to simplify the exposition at the same time, we take

$$A_1 = A_2 = A_3 = A_4 = A_5 = A_8 = A_{11} = A_{13} = A_{14} = A_{15} = 0, \qquad A_{10} = \frac{\mu\,L_c^2}{6}\,, \tag{4.29}$$

in our finite element simulation. Another simplification of the local energy expression seems to be expedient. We assume further on, that with some number $\alpha \in \mathbb{R}$

$$\mu_c = 0\,, \qquad \mu = \alpha\,\mu^{\rm m}\,, \qquad \lambda = \alpha\,\lambda^{\rm m}\,, \quad \alpha \in (0,1)\,. \tag{4.30}$$

For example, $\alpha = 0.9$ means that the large-scale bulk behaviour is assumed to be about 10 percent weaker than the response of a representative volume element (RVE) on the small scale. Taking into account the homogenization formulas derived in (4.13) implies then that

$$\mu_e = \frac{\alpha}{1-\alpha}\,\mu^{\rm m}\,, \qquad \lambda_e = \frac{\alpha}{1-\alpha}\,\lambda^{\rm m}\,. \tag{4.31}$$

Hence in terms of Mindlin's representation we obtain

$$\begin{aligned} &\widehat{\mu} = \frac{1}{\alpha}\mu\,, \quad \widehat{\lambda} = \frac{1}{\alpha}\lambda\,, \\ &b_1 = \lambda_e + \lambda^{\rm m} = \frac{\alpha}{1-\alpha}\,\lambda^{\rm m} + \lambda^{\rm m} = \frac{1}{1-\alpha}\lambda^{\rm m} = \frac{1}{\alpha\,(1-\alpha)}\lambda\,, \\ &b_2 = b_3 = \mu_e + \mu^{\rm m} = \frac{1}{\alpha\,(1-\alpha)}\,\mu\,, \\ &g_1 = -\frac{1}{\alpha}\lambda\,, \quad g_2 = -\frac{1}{\alpha}\mu\,, \end{aligned} \tag{4.32}$$

for given large-scale Lamé moduli μ, λ.

5 Implementation

5.1 Finite Element method for the infinitesimal micromorphic continuum

The implementation of the infinitesimal micromorphic model into a finite element program is illustrated here in the two–dimensional case (plane strain or plane stress). The vector of degrees of freedom attributed to each node is written:

$$[\text{d.o.f}] = [U_1\ U_2\ p_{11}\ p_{22}\ p_{12}\ p_{21}]^T\ . \tag{5.1}$$

The associated generalized strain vector is:

$$\begin{aligned}[\text{grad}] = \quad & [\varepsilon_{11}\ \varepsilon_{22}\ \varepsilon_{33}\ \varepsilon_{12}\ \overline{\varepsilon}_{11}\ \overline{\varepsilon}_{22}\ \overline{\varepsilon}_{33}\ \overline{\varepsilon}_{12}\ \overline{\varepsilon}_{21} \\ & K_{111}\ K_{112}\ K_{121}\ K_{122}\ K_{211}\ K_{212}\ K_{221}\ K_{222}]^T\ .\end{aligned} \tag{5.2}$$

The matrix $[B]$ linking the strain vector to the degrees of freedom reads as follows under plane strain conditions:

$$[\text{grad}] = [B]\ \ [\text{d.o.f}]\,, \quad [B] = \begin{bmatrix} \partial_{x_1} & 0 & 0 & 0 & 0 & 0 \\ 0 & \partial_{x_2} & 0 & 0 & 0 & 0 \\ 0 & 0 & 0 & 0 & 0 & 0 \\ \frac{1}{2}\partial_{x_2} & \frac{1}{2}\partial_{x_1} & 0 & 0 & 0 & 0 \\ \partial_{x_1} & 0 & -1 & 0 & 0 & 0 \\ 0 & \partial_{x_2} & 0 & -1 & 0 & 0 \\ 0 & 0 & 0 & 0 & 0 & 0 \\ \partial_{x_2} & 0 & 0 & 0 & -1 & 0 \\ 0 & \partial_{x_1} & 0 & 0 & 0 & -1 \\ 0 & 0 & \partial_{x_1} & 0 & 0 & 0 \\ 0 & 0 & \partial_{x_2} & 0 & 0 & 0 \\ 0 & 0 & 0 & 0 & \partial_{x_1} & 0 \\ 0 & 0 & 0 & 0 & \partial_{x_2} & 0 \\ 0 & 0 & 0 & 0 & 0 & \partial_{x_1} \\ 0 & 0 & 0 & 0 & 0 & \partial_{x_2} \\ 0 & 0 & 0 & \partial_{x_1} & 0 & 0 \\ 0 & 0 & 0 & \partial_{x_2} & 0 & 0 \end{bmatrix}, \tag{5.3}$$

where $\partial_{x_i} = \partial \cdot /\partial x_i$. Plane strain conditions imply $\varepsilon_{33} = \overline{\varepsilon}_{33} = 0$. In the case of plane stress conditions, ε_{33} and $\overline{\varepsilon}_{33}$ are introduced as additional degrees of freedom shared by each element. The associated reactions are σ_{33} and s_{33}. Plane stress conditions are enforced by prescribing vanishing reaction stresses, but other conditions can also be considered. The generalized stress vector reads:

$$\begin{aligned}[\text{flux}] = \quad & [\sigma_{11}\ \sigma_{22}\ \sigma_{33}\ \sigma_{12}\ s_{11}\ s_{22}\ s_{33}\ s_{12}\ s_{21} \\ & S_{111}\ S_{112}\ S_{121}\ S_{122}\ S_{211}\ S_{212}\ S_{221}\ S_{222}]^T\ .\end{aligned} \tag{5.4}$$

The isotropic elasticity matrix linking the elastic part of the micro–deformation gradient and the third–rank stress tensor is written as:

$$\begin{bmatrix} M_{111} \\ M_{112} \\ M_{121} \\ M_{122} \\ M_{211} \\ M_{212} \\ M_{221} \\ M_{222} \end{bmatrix} = [A] \begin{bmatrix} K_{111} \\ K_{112} \\ K_{121} \\ K_{122} \\ K_{211} \\ K_{212} \\ K_{221} \\ K_{222} \end{bmatrix}, \tag{5.5}$$

where $[A]$ equals

$$\begin{bmatrix} AA & 0 & 0 & A_{1,4,5} & 0 & A_{2,5,8} & A_{1,2,3} & 0 \\ 0 & A_{3,10,14} & A_{2,11,13} & 0 & A_{1,11,15} & 0 & 0 & A_{1,2,3} \\ 0 & A_{2,11,13} & A_{8,10,15} & 0 & A_{5,11,14} & 0 & 0 & A_{2,5,8} \\ A_{1,4,5} & 0 & 0 & A_{4,10,13} & 0 & A_{5,11,14} & A_{1,11,15} & 0 \\ 0 & A_{1,11,15} & A_{5,11,14} & 0 & A_{4,10,13} & 0 & 0 & A_{1,4,5} \\ A_{2,5,8} & 0 & 0 & A_{5,11,14} & 0 & A_{8,10,15} & A_{2,11,13} & 0 \\ A_{1,2,3} & 0 & 0 & A_{1,11,15} & 0 & A_{2,11,13} & A_{3,10,14} & 0 \\ 0 & A_{1,2,3} & A_{2,5,8} & 0 & A_{1,4,5} & 0 & 0 & AA \end{bmatrix}, \tag{5.6}$$

with $AA = 2A_1 + 2A_2 + A_3 + A_4 + 2A_5 + A_8 + A_{10} + 2A_{11} + A_{13} + A_{14} + A_{15}$. The notation $A_{i,j,k} = A_i + A_j + A_k$ is used.

The variational formulation of the micromorphic boundary value problem is a straightforward extension of the classical one:

$$\int_{\Omega} \langle \sigma, \dot{\varepsilon} \rangle + \langle s, \dot{\bar{\varepsilon}} \rangle + \langle S, \dot{K} \rangle \,\mathrm{dV} = \int_{\partial\Omega} \langle t, \dot{u} \rangle + \langle M, \dot{p} \rangle \,\mathrm{dS}\,, \tag{5.7}$$

with the boundary conditions (4.24). The finite element formulation follows from the same discretization of the variational problem as in the classical case.

An analytical solution of a simple boundary value problem for the linear elastic micromorphic continuum is proposed in appendix 7.5, which serves as validation test for the implementation of the model.

5.2 Finite element simulations of hole size effects in metallic foams

One of the early goals of the mechanics of generalized continua was to control the magnitude of stress concentrations at holes, edges or cracks. Indeed, Mindlin analysed the stress concentration coefficient at a hole in a plate in the case of a couple–stress medium [54]. Contrary to the classical situation, the stress concentration factor is found to depend on the relative size of the hole with respect to the value of the characteristic size even if the hole is embedded in an infinite matrix. The analytical solution of the more general problem of the spherical or cylindrical elastic inclusion inside an infinite matrix was solved only recently for infinitesimal-strain Cosserat elasticity [16, 15, 70]. Finite element simulations within the infinitesimal Cosserat framework show that, contrary to the classical situation, the stress–strain state is generally not homogeneous inside a spherical or cylindrical elastic heterogeneity [32]. The stress concentration factor at the equator of a cylindrical hole in an infinite linear elastic Cosserat matrix tends asymptotically to the classical constant value for large enough holes. For holes with a radius close to or smaller than the value of the intrinsic lengths of the Cosserat matrix, the factor is found to decrease. The value for vanishingly small holes tends towards an asymptotic limit that depends on the Cosserat intrinsic length scale and on the additional Cosserat couple modulus $\mu_c \geq 0$. **For strictly positive Cosserat couple modulus $\mu_c > 0$ it remains larger than one, meaning that holes of any size induce stress concentration in a traditional infinitesimal Cosserat medium.** This behavior is illustrated by figure 2.

The strain field around a cylindrical hole in an infinite micromorphic matrix under plane stress conditions is now investigated using the finite element method. The material parameters used for the presented simulations are taken so as to represent large scale samples of nickel foam studied at room temperature in [4, 21]. This corresponds to

$$\mu = 165\,\mathrm{MPa} \qquad \lambda = 110\,\mathrm{MPa}\,, \tag{5.8}$$

in terms of the Lamé constants. We choose the factor $\alpha = 0.9$ appearing in (4.30) and the Cosserat couple modulus $\mu_c = 0$. This implies

$$\begin{aligned} &\widehat{\mu} = \frac{1}{\alpha}\mu = 183.\,\mathrm{MPa}\,, \quad \widehat{\lambda} = \frac{1}{\alpha}\lambda = 122.\,\mathrm{MPa}\,, \quad b_1 = \frac{1}{\alpha\,(1-\alpha)}\lambda = 1222.\,\mathrm{MPa}\,, \\ &b_2 = b_3 = \mu_e + \mu^{\mathrm{m}} = \frac{1}{\alpha\,(1-\alpha)}\,\mu = 1833.\,\mathrm{MPa}\,, \\ &g_1 = -\frac{1}{\alpha}\lambda = -122.\,\mathrm{MPa}\,, \quad g_2 = -\frac{1}{\alpha}\mu = -183.\,\mathrm{MPa}\,, \end{aligned} \tag{5.9}$$

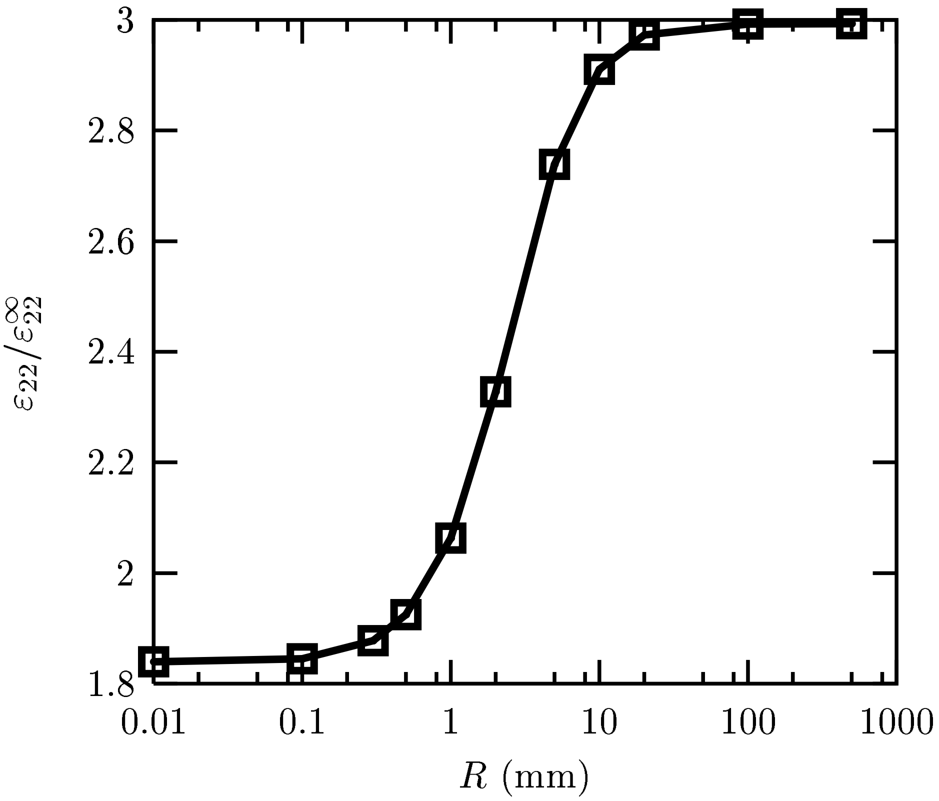

Figure 2: (traditional linear Cosserat response) Strain concentration at the "equator" of a cylindrical hole in an infinite Cosserat medium under tensile loading by the stress ε^{∞} in direction 2. The component plotted is $\varepsilon_{22}/\varepsilon_{22}^{\infty}$. The material properties of the Cosserat equivalent medium representing the nickel foam are taken to be $\mu_e = \mu = 165\,\mathrm{MPa}$, $\lambda_e = \lambda = 110\,\mathrm{MPa}$, $\mu_c = 1000\,\mathrm{MPa}$, $L_c = 1.35\,\mathrm{mm}$.

in terms of Mindlin's representation. The elastic constants b_i act as well as penalty terms that force the relative elastic deformation to remain small. This ensures that the microdeformation is close to the gradient of the displacement field so that the micromorphic model almost degenerates into a second gradient theory [33]. A single additional parameter, namely the characteristic length $L_c > 0$, is introduced in the six–rank tensor A by setting $A_{10} = \frac{\mu L_c^2}{6}$ in Mindlin's representation and $A_1, A_2, \ldots = 0$ for the remaining coefficients. The characteristic length is set to $L_c = 1.35$ mm in the following simulations. Hence

$$A_{10} = \frac{\mu L_c^2}{6} = 50\,\mathrm{MPa}\,\mathrm{mm}^2 . \tag{5.10}$$

This value was identified in the particular case of nickel foam with relative density $\rho^\star/\rho_{Ni} = 0.035$ and mean cell diameter 500 μm. It is in accordance with results of strain field measurements provided in [21].

Figure 3 shows the results of finite element simulations of the tension of a plate with a machined cylindrical hole. Tension is applied along the vertical direction 2 under plane stress conditions. The figure 3a shows the reference strain field ε_{22} around the hole expected in the case of a classical Cauchy continuum. Only the mesh region surrounding the hole is shown. Vertical displacement is applied at the top of the mesh which is not represented in the picture. For such a classical simulation, the size of the hole does not matter. In contrast, the figures 3b and 3c show the strain map ε_{22} around a hole embedded in an infinite linear elastic micromorphic matrix using the values of the elastic properties given by (5.9). The results are given for two hole sizes: $R = 1$ mm and $R = 0.3$ mm respectively. For both computations, the applied strain at infinity ε_{22}^∞ is the same and the material parameters correspond to each other. The size of the hole is the only varying parameter. It clearly appears that the strain field becomes more and more homogeneous when the hole size is reduced. For $R = 0.3$ mm, there is almost no strain concentration at the equator any longer.

For larger and larger holes, we have checked that the classical solution of figure 3a is retrieved when using the micromorphic model. The striking feature of the numerical simulations is that for vanishingly small holes, the micromorphic theory predicts a strictly homogeneous strain field: tiny holes do not introduce any strain fluctuation. This can be seen more quantitatively from the curves of figure 4. The strain profile along the ligament $x_2 = 0$ is plotted for different values of the hole radius ranging from $R = 10$ mm to $R = 0.1$ mm. The curve obtained for $R = 10$ mm is almost identical to the classical result which predicts a stress/strain concentration factor of 3 at the equator ($x_1 = R$) under plane stress conditions. Strain localization decreases for smaller holes. As a result, the strain concentration factor tends to 1 when the hole size tends to zero. This is contrary to the case of the infinitesimal Cosserat continuum (see figure 2). These numerical results cannot currently be compared to analytical solutions which do not seem to be available for a hole in a general linear micromorphic continuum, to the best knowledge of the authors. An analytical solution for the more restricted linear microstretch case has been derived in [18].

The interesting point is that, in a linear elastic micromorphic continuum, there is a limit size below which no geometrical heterogenities can be detected. This limit size sets the resolution of the continuum, in a way similar to the resolution of a microscope. An equivalent parametric study is possible by varying the intrinsic length scale parameter L_c for a fixed radius size R. This enables us in fact to identify the value of the characteristic length that leads to strain concentration around holes only when the holes are sufficiently larger than the cell size.

It must be noted that the finite element simulations were not carried out on one quarter of the sample but for the entire structure, in contrast to the classical case. The reason is that, in spite of the symmetry conditions, it is not possible to know **a priori** what are the boundary conditions p_{11} or p_{22} (or conversely the reactions M_{11} or M_{22}) to be prescribed on the lines $x_1 = 0$ or $x_2 = 0$. This difficulty does not arise for a linear Cosserat continuum since the symmetry conditions imply that the infinitesimal microrotation vanishes at these boundaries. The computation time is therefore increased not only by the larger number of degrees of freedom but also by the fact that the entire specimen must be meshed instead of one quarter. The mesh size in the presented simulations is satisfactory in the sense that convergence is achieved for the generalized stress and strain fields upon mesh refinement, up to a precision better than 1%.

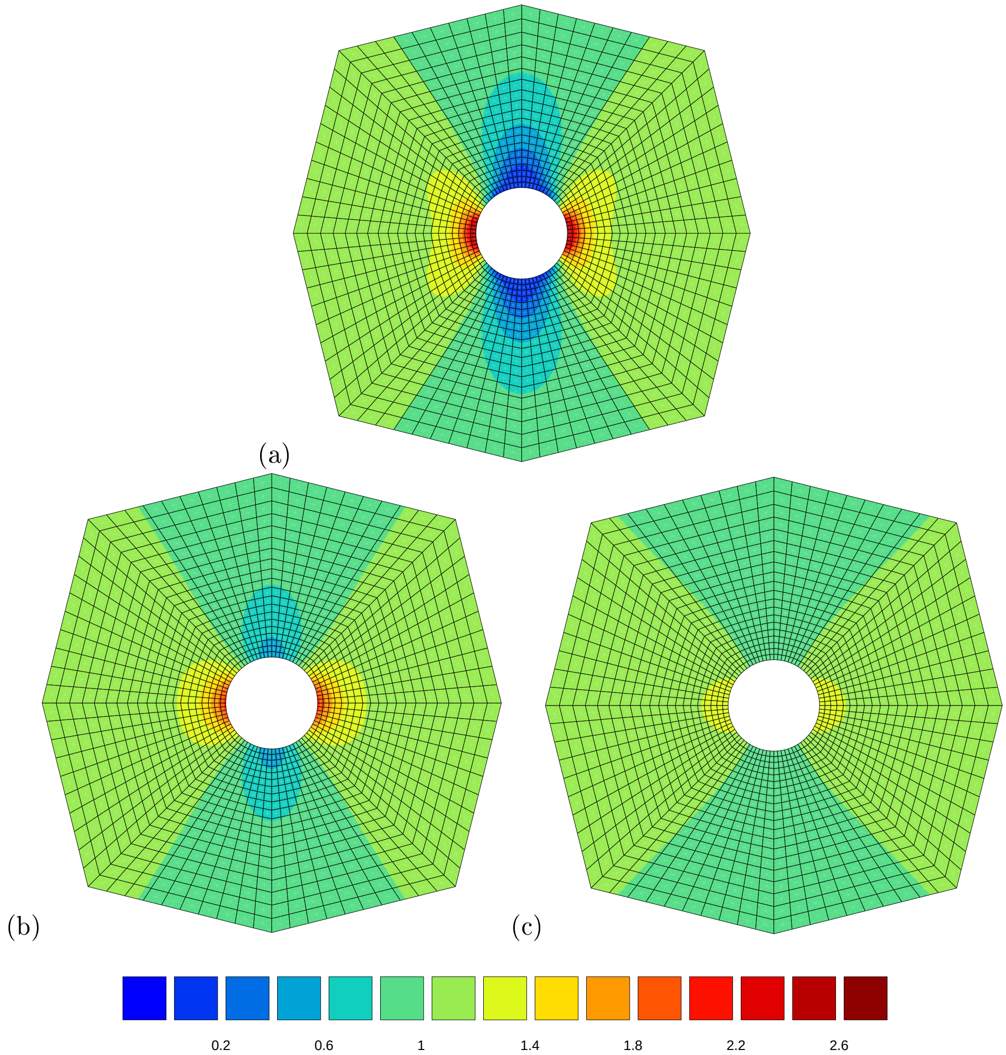

Figure 3: Strain field $\varepsilon_{22}/\varepsilon_{22}^{\infty}$ around a cylindrical hole in an infinite matrix under tensile loading $\varepsilon_{22}^{\infty}$ under plane stress conditions: (a) classical continuum (reference solution), (b) linear elastic micromorphic continuum for a hole radius $R = 1$ mm, (c) linear elastic micromorphic continuum for a hole radius $R = 0.3$ mm. The tensile direction 2 is vertical, the horizontal direction is 1. For the illustration, a magnifcation factor was applied so that the three holes have the same apparent radius. Only the region of the mesh surrounding the hole is shown. The elastic moduli usedfor the simulation are given by (5.9).

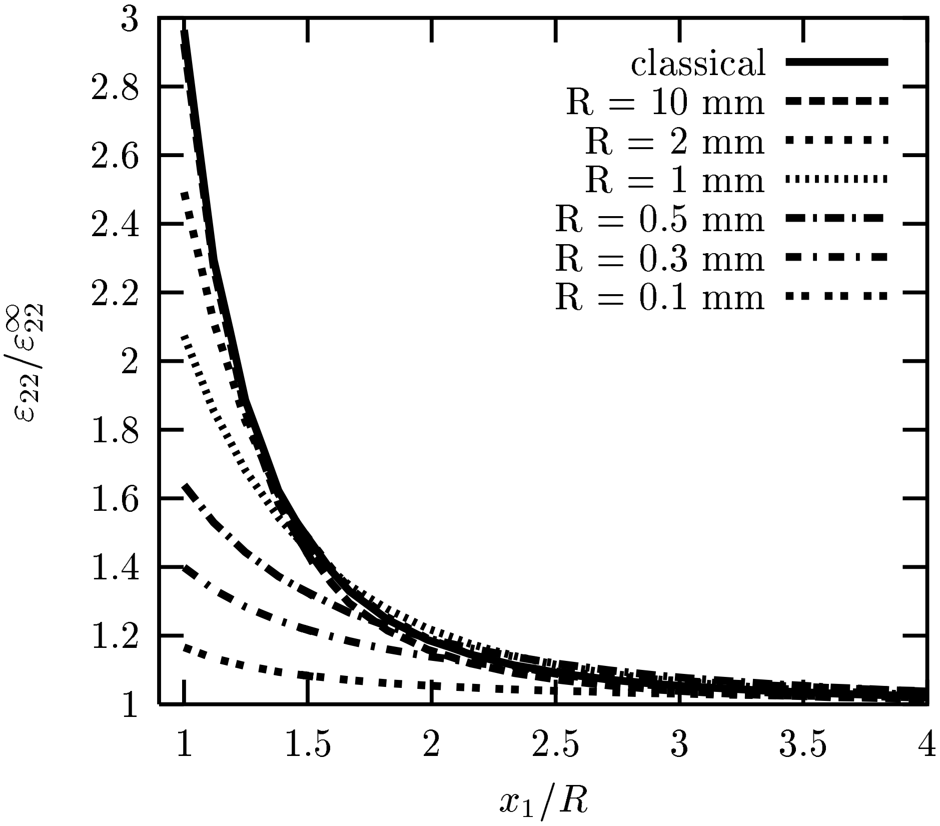

Figure 4: Computed strain profile along the ligament $x_2 = 0$ for the linear micromorphic plate with a cylindrical hole of radius R. The position $x_1 = R$, called "equator" is the location of stress and strain maximum at least for large enough holes. The elastic moduli used for the simulations are given by (5.9).

6 Final remarks

The presented variational finite-strain micromorphic problem fits neatly into the framework of the direct methods of variations. The coercivity part for the deformation is, however, nontrivial and for the value of the Cosserat couple modulus $\mu_c = 0$ additional difficulties arise which can only be circumvented by the use of the generalized Korn's first inequality. In both treated cases I/II, more realistic assumptions on the applied external loads Π are necessary to establish a lower bound for the energy I and a control of the curvature independent of the magnitude of deformation.

Altogether, the quasistatic finite-strain micromorphic theory is established on firm mathematical grounds. With the same methods, the geometrically exact microstretch case can also be treated. An extension of the method to other choices of strain and curvature measures needs to be done, however, this might be a non-trivial task due to certain deficiencies of these measures. The open case III allows for discontinuous macroscopic deformations and might therefore be a model problem allowing to describe fracture.

Our variational framework is ideally suited for subsequent numerical treatment within the finite element method. This is shown by numerically studying the linearized micromorphic model meant to describe the behaviour of nickel foams. In these calculations, the Cosserat couple modulus μ_c is indeed set to zero and the obtained result is contrasted with the response of a traditional infinitesimal Cosserat model with high Cosserat couple modulus μ_c. It seems that the micromorphic model with zero Cosserat couple modulus $\mu_c = 0$ is indeed sufficient to capture the underlying physics. The importance of the characteristic size of the cells on the response of the structure is clearly revealed.

A more accurate description for the foam is clearly needed but this requires an extension of the presented elastic model towards a consistent elastoplastic constitutive setting as proposed e.g in [33] for infinitesimal and finite deformations. The involved characteristic length(s) can be identified using an inverse approach from the strain field measurements. An alternative way is to derive the effective properties of an equivalent homogeneous micromorphic medium from the knowledge of the detailed cell morphology based on homogenization procedures that are now available for generalized continua [29].

References

[1] E.L. Aero and E.V. Kuvshinskii. Fundamental equations of the theory of elastic media with rotationally interacting particles. *Soviet Physics-Solid State*, 2:1272–1281, 1961.

[2] S. Antman. *Nonlinear Problems of Elasticity*, volume 107 of *Applied Mathematical Sciences.* Springer, Berlin, 1995.

[3] J. Appell and P. Zabrejko. *Nonlinear Superposition Operators.*, volume 95 of *Cambridge Tracts in Mathematics.* Cambridge University Press, Cambridge, 1990.

[4] X. Badiche, S. Forest, T. Guibert, Y. Bienvenu, J.-D. Bartout, P. Ienny, M. Croset, and H. Bernet. Mechanical properties and non-homogeneous deformation of open-cell nickel foams : application of the mechanics of cellular solids and of porous materials. *Mat. Science and Engineering A*, A289:276–288, 2000.

[5] A. Bertram and B. Svendsen. On material objectivity and reduced constitutive equations. *Arch. Mech.*, 53:653–675, 2001.

[6] J.-S. Blazy, A. Marie-Louise, S. Forest, Y. Chastel, A. Pineau, A. Awade, C. Grolleron, and F. Moussy. Deformation and fracture of aluminium foams under proportional and non proportional multi–axial loading: Statistical analysis and size effect. *Int. J. Mech. Sci.*, 46:217–244, 2004.

[7] G. Capriz. *Continua with Microstructure.* Springer, Heidelberg, 1989.

[8] G. Capriz and P. Podio Guidugli. Formal structure and classification of theories of oriented media. *Ann. Mat. Pura Appl., Ser. IV*, 115:17–39, 1977.

[9] G. Capriz and P. Podio-Guidugli. Structured continua from a Lagrangian point of view. *Ann. Mat. Pura Appl. Ser. IV*, 135:1–25, 1983.

[10] P. Cermelli and M.E. Gurtin. On the characterization of geometrically necessary dislocations in finite plasticity. *J. Mech. Phys. Solids*, 49:1539–1568, 2001.

[11] C. Chen and N.A. Fleck. Size effects in the constrained deformation of metallic foams. *J. Mech. Phys. Solids*, 50:955–977, 2002.

[12] W. Chen and J. Jost. A Riemannian version of Korn's inequality. *Calculus Variations.*, 14:517–530, 2002.

[13] Y. Chen and J.D. Lee. Connecting molecular dynamics to micromorphic theory. I. Instantaneous and averaged mechanical variables. *Physica A*, 322:359–376, 2003.

[14] Y. Chen and J.D. Lee. Connecting molecular dynamics to micromorphic theory. II. Balance laws. *Physica A*, 322:376–392, 2003.

[15] Z.-Q. Cheng and L.-H. He. Micropolar elastic fields due to a circular cylindrical inclusion. *Int. J. Engng Sci.*, 35:659–668, 1997.

[16] Z.-Q. Cheng and L.-H.He. Micropolar elastic fields due to a spherical inclusion. *Int. J. Engng Sci.*, 33:389–397, 1995.

[17] P.G. Ciarlet. *Three-Dimensional Elasticity*, volume 1 of *Studies in Mathematics and its Applications.* Elsevier, Amsterdam, first edition, 1988.

[18] S. De Cicco. Stress concentration effects in microstretch elastic bodies. *Int. J.. Engng. Sci.*, 41:187–199, 2003.

[19] E. Cosserat and F. Cosserat. *Théorie des corps déformables.* Librairie Scientifique A. Hermann et Fils (Theory of deformable bodies, NASA TT F-11 561, 1968), Paris, 1909.

[20] A. Dietsche, P. Steinmann, and K. William. Micropolar elastoplasticity and its role in localization. *Int. J. Plasticity*, 9:813–831, 1993.

[21] T. Dillard. *Comportement mécanique et rupture des mousses de nickel : caractérisation 3D, mesures de champs et simulation numérique.* Phd. thesis, Ecole des Mines de Paris, 2004.

[22] G. Duvaut. Elasticité linéaire avec couples de contraintes. Théorémes d'existence. *J. Mec. Paris*, 9:325–333, 1970.

[23] W. Ehlers, S. Diebels, and W. Volk. Deformation and compatibilty for elasto-plastic micropolar materials with applications to geomechanical problems. In A. Bertram and F. Sidoroff, editors, *Mechanics of Materials with Intrinsic Length Scale: Physics, Experiments, Modelling and Applications.*, Journal Physique IV France 8, pages 127–134. EDP Sciences, France, 1998.

[24] A. C. Eringen. *Microcontinuum Field Theories.* Springer, Heidelberg, 1999.

[25] A.C. Eringen. Theory of Micropolar Elasticity. In H. Liebowitz, editor, *Fracture. An advanced treatise.*, volume II, pages 621–729. Academic Press, New York, 1968.

[26] A.C. Eringen and C.B. Kafadar. Polar Field Theories. In A.C. Eringen, editor, *Continuum Physics*, volume IV: Polar and Nonlocal Field Theories, pages 1–73. Academic Press, New York, 1976.

[27] A.C. Eringen and E.S. Suhubi. Nonlinear theory of simple micro-elastic solids. *Int. J. Eng. Sci.*, 2:189–203, 1964.

[28] N.A. Fleck, O.B. Olurin, C. Chen, and M.F. Ashby. The effect of hole size upon the strength of metallic and polymeric foams. *J. Mech. Phys. Solids*, 49:2015–2030, 2001.

[29] S. Forest. Homogenization methods and the mechanics of generalized continua–Part 2. *Theoretical and Applied Mechanics*, 28–29:113–143, 2002.

[30] S. Forest, F. Barbe, and G. Cailletaud. Cosserat modelling of size effects in the mechanical behaviour of polycrystals and multi-phase materials. *Int. J. Solids Struct.*, 37:7105–7126, 2000.

[31] S. Forest, G. Cailletaud, and R. Sievert. A Cosserat theory for elastoviscoplastic single crystals at finite deformation. *Arch. Mech.*, 49(4):705–736, 1997.

[32] S. Forest, R. Dendievel, and G.R. Canova. Estimating the overall properties of heterogeneous cosserat materials. *Mod. Simul. Mater. Sci. Eng.*, 7:829–840, 1999.

[33] S. Forest and R. Sievert. Elastoviscoplastic constitutive frameworks for generalized continua. *Acta Mech.*, 160:71–111, 2003.

[34] R.D. Gauthier. Experimental investigations on micropolar media. In O. Brulin and R.K.T. Hsieh, editors, *Mechanics of Micropolar Media*, pages 395–463. CISM Lectures, World Scientific, Singapore, 1982.

[35] P. Germain. The method of virtual power in continuum mechanics. Part 2 : Microstructure. *SIAM J. Appl. Math.*, 25:556–575, 1973.

[36] V. Gheorghita. On the existence and uniqueness of solutions in linear theory of Cosserat elasticity. I. *Arch. Mech.*, 26:933–938, 1974.

[37] V. Gheorghita. On the existence and uniqueness of solutions in linear theory of Cosserat elasticity. II. *Arch. Mech.*, 29:355–358, 1974.

[38] L.J. Gibson and M.F. Ashby. *Cellular solids.* Cambridge University Press, 1998.

[39] W. Günther. Zur Statik und Kinematik des Cosseratschen Kontinuums. *Abh. Braunschweigische Wiss. Gesell.*, 10:195–213, 1958.

[40] P. Grammenoudis. *Mikropolare Plastizität.* Ph.D-Thesis, Department of Mechanics. TU Darmstadt, http://elib.tu-darmstadt.de/diss/000312, 2003.

[41] A.E. Green and R.S. Rivlin. Multipolar continuum mechanics. *Arch. Rat. Mech. Anal.*, 17:113–147, 1964.

[42] J.L. Grenestedt. Effective elastic behavior of some models for "perfect"cellular solids. *Int. J. Solids Struct.*, 36:1471–1501, 1999.

[43] M.E. Gurtin and P. Podio-Guidugli. On the formulation of mechanical balance laws for structured continua. *Z. Angew. Math. Phys.*, 43:181–190, 1992.

[44] I. Hlavacek and M. Hlavacek. On the existence and uniqueness of solutions and some variational principles in linear theories of elasticity with couple-stresses. I: Cosserat continuum. II: Mindlin's elasticity with micro-structure and the first strain gradient. *J. Apl. Mat.*, 14:387–426, 1969.

[45] D. Hofer. *Simulation von Größeneffekten mit mikromorphen Theorien.* Ph.D-Thesis, Department of Mechanics. TU Darmstadt, http://elib.tu-darmstadt.de, 2003.

[46] D. Iesan. Existence theorems in micropolar elastostatics. *Int. J. Eng. Sci.*, 9:59, 1971.

[47] D. Iesan and A. Pompei. On the equilibrium theory of microstretch elastic solids. *Int. J. Eng. Sci.*, 33:399–410, 1995.

[48] D. Iesan and R. Quintanilla. Existence and continuous dependence results in the theory of microstretch elastic bodies. *Int. J. Eng. Sci.*, 32:991–1001, 1994.

[49] D. Iesan and A. Scalia. On Saint-Venants principle for microstretch elastic bodies. *Int. J. Eng. Sci.*, 35:1277–1290, 1997.

[50] M.M. Iordache and K. William. Localized failure analysis in elastoplastic Cosserat continua. *Comp. Meth. Appl. Mech. Engrg.*, 151:559–586, 1998.

[51] E. Kröner. *Mechanics of Generalized Continua.* Proceedings of the IUTAM-Symposium on the generalized Cosserat continuum and the continuum theory of dislocations with applications in Freudenstadt, 1967. Springer, Heidelberg, 1968.

[52] J.E. Marsden and J.R. Hughes. *Mathematical Foundations of Elasticity.* Prentice-Hall, Englewood Cliffs, New Jersey, 1983.

[53] G.A. Maugin. On the structure of the theory of polar elasticity. *Phil. Trans. Roy. Soc. London A*, 356:1367–1395, 1998.

[54] R.D. Mindlin. Influence of couple–stresses on stress concentrations. *Experimental Mechanics*, 3:1–7, 1962.

[55] R.D. Mindlin. Micro-structure in linear elasticity. *Arch. Rat. Mech. Anal.*, 16:51–77, 1964.

[56] R.D. Mindlin and H.F. Tiersten. Effects of couple stresses in linear elasticity. *Arch. Rat. Mech. Anal.*, 11:415–447, 1962.

[57] A.I. Murdoch. Objectivity in classical continuum physics: a rational for discarding the 'principle of invariance under superposed rigid body motions' in favour of purely objective considerations. *Cont. Mech. Thermo.*, 15:309–320, 2003.

[58] P. Neff. On Korn's first inequality with nonconstant coefficients. *Proc. Roy. Soc. Edinb.*, 132A:221–243, 2002.

[59] P. Neff. Finite multiplicative plasticity for small elastic strains with linear balance equations and grain boundary relaxation. *Cont. Mech. Thermodynamics*, 15(2)(DOI 10.1007/s00161-002-0190-x):161–195, 2003.

[60] P. Neff. A geometrically exact micromorphic elastic solid. Modelling and existence of minimizers. *Preprint 2318, http://wwwbib.mathematik.tu-darmstadt.de/Math-Net/Preprints/Listen/pp04.html, submitted to Calculus of Variations*, 2/2004.

[61] P. Neff. Finite multiplicative elastic-viscoplastic Cosserat micropolar theory for polycrystals with grain rotations. Modelling and mathematical analysis. *Preprint 2297, http://wwwbib.mathematik.tu-darmstadt.de/Math-Net/Preprints/Listen/pp03.html, submitted*, 9/2003.

[62] W. Nowacki. *Theory of Asymmetric Elasticity.* Pergamon Press, Oxford, 1986.

[63] P.R. Onck, E.W. Andrews, and L.J. Gibson. Size effects in ductile cellular solids. Part I : Modeling. *Int. J. Mech. Sci.*, 43:681–699, 2001.

[64] N. Oshima. Dynamics of granular media. In K. Kondo, editor, *Memoirs of the Unifying Study of the Basic Problems in Engineering Science by Means of Geometry*, volume 1, Division D-VI, pages 111–120 (563–572). Gakujutsu Bunken Fukyo-Kai, 1955.

[65] P. Podio-Guidugli and G. Vergara Caffarelli. Extreme elastic deformations. *Arch. Rat. Mech. Anal.*, 115:311–328, 1991.

[66] W. Pompe. Korn's first inequality with variable coefficients and its generalizations. *Comment. Math. Univ. Carolinae*, 44,1:57–70, 2003.

[67] F. Pradel and K. Sab. Homogenization of discrete media. *Journal de Physique IV*, 8:Pr8–317–324, 1998.

[68] C. Sansour. *Ein einheitliches Konzept verallgemeinerter Kontinua mit Mikrostruktur unter besonderer Berücksichtigung der finiten Viskoplastizität.* Habilitation-Thesis, Shaker-Verlag, Aachen, 1999.

[69] H. Schaefer. Das Cosserat-Kontinuum. *ZAMM*, 47:485–498, 1967.

[70] P. Sharma and A. Dasgupta. Scale–dependent average elastic fields of spherical and cylindrical inhomogeneities in micropolar medium and overall properties. Technical Report 2001CRD130, GE Research and Development Center, New York, USA, 2001.

[71] P. Steinmann. A micropolar theory of finite deformation and finite rotation multiplicative elastoplasticity. *Int. J. Solids Structures*, 31(8):1063–1084, 1994.

[72] P. Steinmann. A unifying treatise of variational principles for two types of micropolar continua. *Acta Mech.*, 121:215–232, 1997.

[73] B. Svendsen and A. Bertram. On frame-indifference and form-invariance in constitutive theory. *Acta Mechanica*, 132:195–207, 1997.

[74] R.A. Toupin. Elastic materials with couple stresses. *Arch. Rat. Mech. Anal.*, 11:385–413, 1962.

[75] R.A. Toupin. Theory of elasticity with couple stresses. *Arch. Rat. Mech. Anal.*, 17:85–112, 1964.

[76] C. Truesdell and W. Noll. The non-linear field theories of mechanics. In S. Fluegge, editor, *Handbuch der Physik*, volume III/3. Springer, Heidelberg, 1965.

[77] J.F. Yang and R.S.Lakes. Transient study of couple stress effects in compact bone : torsion. *J. of Biomech. Engng.*, 103:275–279, 1981.

7 Appendix

7.1 Notation

Let $\Omega \subset \mathbb{R}^3$ be a bounded domain with Lipschitz boundary $\partial\Omega$ and let Γ be a smooth subset of $\partial\Omega$ with non-vanishing 2-dimensional Hausdorff measure. For $a, b \in \mathbb{R}^3$ we let $\langle a, b\rangle_{\mathbb{R}^3}$ denote the scalar product on $\mathbb{R}^3$ with associated vector norm $\|a\|^2_{\mathbb{R}^3} = \langle a, a\rangle_{\mathbb{R}^3}$. We denote by $\mathbb{M}^{3\times 3}$ the set of real 3×3 second order tensors, written with capital letters and by $\mathfrak{T}(3)$ the set of all third order tensors. The standard Euclidean scalar product on $\mathbb{M}^{3\times 3}$ is given by $\langle X, Y\rangle_{\mathbb{M}^{3\times 3}} = \operatorname{tr}\left[XY^T\right]$, and thus the Frobenius tensor norm is $\|X\|^2 = \langle X, X\rangle_{\mathbb{M}^{3\times 3}}$. In the following we omit the index $\mathbb{R}^3, \mathbb{M}^{3\times 3}$. The identity tensor on $\mathbb{M}^{3\times 3}$ will be denoted by $1\!\!1$, so that $\operatorname{tr}[X] = \langle X, 1\!\!1\rangle$. We let Sym and PSym denote the symmetric and positive definite symmetric tensors respectively. We adopt the usual abbreviations of Lie-group theory, i.e., $\mathrm{GL}(3,\mathbb{R}) := \{X \in \mathbb{M}^{3\times 3} \; |\det[X] \neq 0\}$ the general linear group, $\mathrm{SL}(3,\mathbb{R}) := \{X \in \mathrm{GL}(3,\mathbb{R}) \; |\det[X] = 1\}$, $\mathrm{O}(3) := \{X \in \mathrm{GL}(3,\mathbb{R}) \mid X^TX = 1\!\!1\}$, $\mathrm{SO}(3,\mathbb{R}) := \{X \in \mathrm{GL}(3,\mathbb{R}) \; |X^TX = 1\!\!1, \; \det[X] = 1\}$ with corresponding Lie-algebras $\mathfrak{so}(3) := \{X \in \mathbb{M}^{3\times 3} \; |X^T = -X\}$ of skew symmetric tensors and $\mathfrak{sl}(3) := \{X \in \mathbb{M}^{3\times 3} \; |\operatorname{tr}[X] = 0\}$ of traceless tensors. We set $\operatorname{sym}(X) = \frac{1}{2}(X^T + X)$ and $\operatorname{skew}(X) = \frac{1}{2}(X - X^T)$ such that $X = \operatorname{sym}(X) + \operatorname{skew}(X)$. For $X \in \mathbb{M}^{3\times 3}$ we set for the deviatoric part $\operatorname{dev} X = X - \frac{1}{3}\operatorname{tr}[X]\,1\!\!1 \in \mathfrak{sl}(3)$ and for vectors $\xi, \eta \in \mathbb{R}^n$ we have the tensor product $(\xi \otimes \eta)_{ij} = \xi_i\,\eta_j$. The operator $\operatorname{axl} : \mathfrak{so}(3,\mathbb{R}) \mapsto \mathbb{R}^3$ is the canonical identification. We write the polar decomposition in the form $F = RU = \operatorname{polar}(F)U$ with $R = \operatorname{polar}(F)$ the orthogonal part of F. For a second order tensor X we define the third order tensor $\mathfrak{h} = \mathrm{D}_x X(x) = (\nabla(X(x).e_1), \nabla(X(x).e_2), \nabla(X(x).e_3)) = (\mathfrak{h}^1, \mathfrak{h}^2, \mathfrak{h}^3) \in \mathbb{M}^{3\times 3} \times \mathbb{M}^{3\times 3} \times \mathbb{M}^{3\times 3}$. For third order tensors $\mathfrak{h} \in \mathfrak{T}(3)$ we set $\|\mathfrak{h}\|^2 = \sum_{i=1}^3 \|\mathfrak{h}^i\|^2$ together with $\operatorname{sym}(\mathfrak{h}) := (\operatorname{sym}\mathfrak{h}^1, \operatorname{sym}\mathfrak{h}^2, \operatorname{sym}\mathfrak{h}^3)$ and $\operatorname{tr}[\mathfrak{h}] := (\operatorname{tr}\left[\mathfrak{h}^1\right], \operatorname{tr}\left[\mathfrak{h}^2\right], \operatorname{tr}\left[\mathfrak{h}^3\right]) \in \mathbb{R}^3$. Moreover, for any second order tensor X we define $X\cdot\mathfrak{h} := (X\mathfrak{h}^1, X\mathfrak{h}^2, X\mathfrak{h}^3)$ and $\mathfrak{h}\cdot X$ correspondingly. Quantities with a bar, e.g. the micropolar rotation $\overline{R}_p$, represent the micropolar replacement of the corresponding classical continuum rotation R. In general we work in the context of nonlinear, finite elasticity. For the total deformation $\varphi \in C^1(\overline{\Omega}, \mathbb{R}^3)$ we have the deformation gradient $F = \nabla\varphi \in C(\overline{\Omega}, \mathbb{M}^{3\times 3})$ and we use ∇ in general only for column-vectors in $\mathbb{R}^3$. Furthermore, $S_1(F)$ and $S_2(F)$ denote the first and second Piola Kirchhoff stress tensors, respectively. Total time derivatives are written $\frac{\mathrm{d}}{\mathrm{dt}}X(t) = \dot{X}$. The first and second differential of a scalar valued function $W(F)$ are written $D_F W(F).H$ and $D_F^2 W(F).(H,H)$, respectively. Sometimes we use also $\partial_X W(X)$ to denote the first derivative of W with respect to X. We employ the standard notation of Sobolev spaces, i.e. $L^2(\Omega), H^{1,2}(\Omega), H_\circ^{1,2}(\Omega)$, which we use indifferently for scalar-valued functions as well as for vector-valued and tensor-valued functions. Moreover, we set $\|X\|_\infty = \sup_{x\in\Omega}\|X(x)\|$. For $X \in C^1(\overline{\Omega}, \mathbb{M}^{3\times3})$ we define $\operatorname{Curl} X(x)$ and $\operatorname{Div} X(x)$ as the operation curl and Div applied row wise, respectively. For $\mathfrak{h} \in \mathfrak{T}(3)$ we define $\operatorname{Div}\mathfrak{h} = \left(\operatorname{Div}\mathfrak{h}^1 | \operatorname{Div}\mathfrak{h}^2 | \operatorname{Div}\mathfrak{h}^3\right)^T \in \mathbb{M}^{3\times3}$. We define $H_\circ^{1,2}(\Omega,\Gamma) := \{\phi \in H^{1,2}(\Omega) \mid \phi_{|_\Gamma} = 0\}$, where $\phi_{|_\Gamma} = 0$ is to be understood in the sense of traces and by $C_0^\infty(\Omega)$ we denote infinitely differentiable functions with compact support in Ω. We use capital letters to denote possibly large positive constants, e.g. C^+, K and lower case letters to denote possibly small positive constants, e.g. c^+, d^+. The smallest eigenvalue of a positive definite symmetric tensor P is abbreviated by $\lambda_{\min}(P)$. Finally, w.r.t. abbreviates with respect to.

7.2 The coercivity inequality

The decisive analytical tool for the treatment of case II (super-critical) is the following new non-trivial inequality establishing coercivity:

Theorem 7.1 (Extended 3D-Korn's first inequality)
Let $\Omega \subset \mathbb{R}^3$ be a bounded Lipschitz domain and let $\Gamma \subset \partial\Omega$ be a smooth part of the boundary with non vanishing 2-dimensional Hausdorff measure. Define $H_\circ^{1,2}(\Omega,\Gamma) := \{\phi \in H^{1,2}(\Omega) \mid \phi_{|_\Gamma} = 0\}$ and let $F_p, F_p^{-1} \in C^1(\overline{\Omega}, \mathrm{GL}(3,\mathbb{R}))$. Moreover suppose that $\operatorname{Curl} F_p \in C^1(\overline{\Omega}, \mathbb{M}^{3\times3})$. Then

$$\exists\, c^+ > 0\ \forall\, \phi \in H_\circ^{1,2}(\Omega,\Gamma): \quad \|\nabla\phi F_p^{-1}(x) + F_p^{-T}(x)\nabla\phi^T\|^2_{L^2(\Omega)} \geq c^+\ \|\phi\|^2_{H^{1,2}(\Omega)}\,.$$

Proof. The proof has been presented in [58]. ■

Remark 7.2
Note that for $F_p = \nabla\Theta$ we would only have to deal with the classical Korn's inequality evaluated on the transformed domain $\Theta(\Omega)$. However, in general, F_p is **incompatible** *giving rise to a* **non-Riemannian manifold** *structure. Compare this to [10] for an interpretation and the physical relevance of the volume dislocation density tensor $\operatorname{Curl} F_p$. A* **Riemannian** *version of Korn's inequality has also been given in [12].*

Motivated by the investigations in [58] it has been shown recently by Pompe [66] that the extended Korn's inequality can be viewed as a special case of a general class of coercivity inequalities for quadratic forms. He was able to show that indeed $F_p, F_p^{-1} \in C(\overline{\Omega}, \mathrm{GL}(3,\mathbb{R}))$ is sufficient for (7.1) to hold without any condition on the compatibility.

However, taking the special structure of the extended Korn's inequality again into account, work in progress suggests that continuity is not really necessary: instead $F_p, F_p^{-1} \in L^\infty(\Omega, \mathrm{GL}(3,\mathbb{R}))$ and $\operatorname{Curl} F_p \in L^{3+\delta}(\Omega)$ should suffice, whereas $F_p, F_p^{-1} \in L^\infty(\Omega, \mathrm{GL}(3,\mathbb{R}))$ alone is not sufficient, see the counterexample presented in [66]. This possible improvement has no consequences for the analysis, however.

In view of the important role of the extended Korn's first inequality let us agree in saying that an inhomogeneous material characterized by a free energy density $W : \mathbb{R}^3 \times \mathbb{M}^{3\times3} \mapsto \mathbb{R}$ is **elastically pre-stable**, whenever

$$\begin{aligned}
&\exists\, H \in \mathbb{M}^{3\times3},\ H \neq 0: \quad D_F^2 W(x,F).(H,H) = 0 \quad \text{and} \\
&\exists\, c^+ > 0\ \exists\, G \in \mathrm{GL}^+(3,\mathbb{R})\ \forall\, H \in \mathbb{M}^{3\times3}: \ D_F^2 W(x,F).(H,H) \geq c^+\|G(x)^T H + H^T G(x)\|^2\,.
\end{aligned} \tag{7.1}$$

In this terminology, infinitesimal classical elasticity is pre-stable with $G = 1\!\!1$ and the extended Korn's first inequality links the smoothness of G to the positive definiteness of the elastic tangent stiffness tensor.

7.3 Derivation of the geometrically exact micromorphic balance equations

The balance equations are obtained as for the micro-incompressible case with the only provision that we can take as variation for $U_p \in \mathrm{PSym}$ the following expression

$$\frac{\mathrm{d}}{\mathrm{dt}} U_p = T\,U_p, \quad T \in \mathrm{Sym}(3)\,, \tag{7.2}$$

instead of $T \in \mathfrak{sl}(3,\mathbb{R}) \cap \mathrm{Sym}(3)$ for the micro-incompressible case based on $\overline{U}_p$. Note that any value of the differential $\frac{\mathrm{d}}{\mathrm{dt}} U_p$ can be obtained as $\frac{\mathrm{d}}{\mathrm{dt}} U_p = T\,U_p$ for some $T \in \mathrm{Sym}(3)$ while $T\,U_p$ is not necessarily symmetric if T is symmetric.

7.4 Derivation of the geometrically exact micromorphic balance equations in the micro-incompressible case

Introducing a constraint nonlinear manifold like $\mathrm{SL}(3,\mathbb{R})$ for the micro-incompressible case complicates the derivation of the balance equations considerably.

The derivation of the force balance equation remains straight forward, however. Since we can write $\overline{P} = \overline{R}_p \cdot \overline{U}_p$ and $\overline{R}_p, \overline{U}_p$ can be prescribed arbitrarily, we may realize the variation of $\overline{P}$ through independent variation of the orthogonal and isochoric stretch part:

$$\overline{P} = \overline{R}_p \cdot \overline{U}_p \Rightarrow \frac{\mathrm{d}}{\mathrm{dt}}\overline{P} = \left[\frac{\mathrm{d}}{\mathrm{dt}}\overline{R}_p\right]\overline{U}_p + \overline{R}_p\left[\frac{\mathrm{d}}{\mathrm{dt}}\overline{U}_p\right]. \tag{7.3}$$

Now take either $\frac{\mathrm{d}}{\mathrm{dt}}\overline{U}_p = 0$ or $\frac{\mathrm{d}}{\mathrm{dt}}\overline{R}_p = 0$. In the first case, we have the variation

$$\frac{\mathrm{d}}{\mathrm{dt}}\overline{P} = \left[\frac{\mathrm{d}}{\mathrm{dt}}\overline{R}_p\right]\overline{U}_p = A\,\overline{R}_p\,\overline{U}_p = A\,\overline{P}, \quad A \in \mathfrak{so}(3,\mathbb{R})\,, \text{arbitrary}\,, \tag{7.4}$$

and in the second case we have

$$\frac{\mathrm{d}}{\mathrm{dt}}\overline{P} = \overline{R}_p\left[\frac{\mathrm{d}}{\mathrm{dt}}\overline{U}_p\right] = \overline{R}_p\,T\,\overline{U}_p\,,\quad T\in\mathfrak{sl}(3,\mathbb{R})\cap\mathrm{Sym}(3)\,. \tag{7.5}$$

For the first case, we consider simultaneously in each space point a one parameter group of microdeformations $\frac{\mathrm{d}}{\mathrm{dt}}\hat{P}(x,t)=A(x,t)\cdot\hat{P}(x,t)$, $\hat{P}(x,0)=\overline{P}(x)$, $A\in C_0^\infty(\Omega,\mathfrak{sl}(3,\mathbb{R}))$. The corresponding stationarity condition is obtained from
$\frac{\mathrm{d}}{\mathrm{dt}}_{|t=0}I(\varphi,\hat{P}(x,t))=0$. This yields three terms: the derivatives involving $W_{\mathrm{mp}}(F,\overline{P})$ and $\Pi(\overline{P})$ are straightforward, using the definition of the one parameter group, and yield

$$\begin{aligned}\frac{\mathrm{d}}{\mathrm{dt}}_{|t=0}\Pi(\hat{P}(x,t)) &= \langle D_{\overline{P}}\Pi(\hat{P}(x,t),\frac{\mathrm{d}}{\mathrm{dt}}\hat{P}(x,t)\rangle = \langle D_{\overline{P}}\Pi(\hat{P}(x,t),A(x,t)\cdot\hat{P}(x,t)\rangle\\ &= \langle D_{\overline{P}}\Pi(\overline{P})\overline{P}^T,A(x,t)\rangle\\ &= \langle D_{\overline{P}}\Pi(\overline{P})\overline{U}_p\overline{R}_p^T,A(x,t)\rangle = \langle\overline{R}_p\overline{R}_p^T\,D_{\overline{P}}\Pi(\overline{P})\overline{U}_p\overline{R}_p^T,A(x,t)\rangle\\ &= \langle\overline{R}_p\,\mathrm{skew}\left(\overline{R}_p^T\,D_{\overline{P}}\Pi(\overline{P})\overline{U}_p\right)\overline{R}_p^T,A(x,t)\rangle\,,\end{aligned}\tag{7.6}$$

and

$$\begin{aligned}&\frac{\mathrm{d}}{\mathrm{dt}}_{|t=0}W_{\mathrm{mp}}(F,\hat{P}(x,t)) = \langle D_{\overline{U}}W_{\mathrm{mp}}(\overline{U},\overline{U}_p),\frac{\mathrm{d}}{\mathrm{dt}}\overline{U}\rangle\\ &= \langle D_{\overline{U}}W_{\mathrm{mp}}(\overline{U},\overline{U}_p),\frac{\mathrm{d}}{\mathrm{dt}}[\hat{P}^{-1}F]\rangle = \langle D_{\overline{U}}W_{\mathrm{mp}}(\overline{U},\overline{U}_p),[\frac{\mathrm{d}}{\mathrm{dt}}\hat{P}^{-1}]F\rangle\\ &= \langle D_{\overline{U}}W_{\mathrm{mp}}(\overline{U},\overline{U}_p),-\hat{P}^{-1}[\frac{\mathrm{d}}{\mathrm{dt}}\hat{P}]\hat{P}^{-1}F\rangle = -\langle D_{\overline{U}}W_{\mathrm{mp}}(\overline{U},\overline{U}_p),\hat{P}^{-1}[\frac{\mathrm{d}}{\mathrm{dt}}\hat{P}]\overline{U}\rangle\\ &= -\langle D_{\overline{U}}W_{\mathrm{mp}}(\overline{U},\overline{U}_p),\hat{P}^{-1}A(x,t)\cdot\hat{P}(x,t)\overline{U}\rangle = -\langle D_{\overline{U}}W_{\mathrm{mp}}(\overline{U},\overline{U}_p)\overline{U}^T,\hat{P}^{-1}A(x,t)\cdot\hat{P}(x,t)\rangle\\ &= -\langle\hat{P}^{-T}D_{\overline{U}}W_{\mathrm{mp}}(\overline{U},\overline{U}_p)\overline{U}^T\hat{P}^T,A(x,t)\rangle = -\langle\overline{R}_p\overline{U}_p^{-1}D_{\overline{U}}W_{\mathrm{mp}}(\overline{U},\overline{U}_p)\overline{U}^T\overline{U}_p\overline{R}_p^T,A(x,t)\rangle\\ &= -\langle\overline{R}_p\,\mathrm{skew}\left(\overline{U}_p^{-1}D_{\overline{U}}W_{\mathrm{mp}}(\overline{U},\overline{U}_p)\overline{U}^T\overline{U}_p\right)\overline{R}_p^T,A(x,t)\rangle\\ &= -\langle\overline{R}_p\,\mathrm{skew}\left(\overline{U}_p^{-1}D_{\overline{U}}W_{\mathrm{mp}}(\overline{U},\overline{U}_p)\overline{U}^T\overline{U}_p^T\right)\overline{R}_p^T,A(x,t)\rangle\end{aligned}\tag{7.7}$$

Here, $\langle\cdot,\cdot\rangle$ means additionally integration w.r.t. x. For the term containing the curvature part, we note

$$\begin{aligned}&\frac{\mathrm{d}}{\mathrm{dt}}_{|t=0}\int_\Omega W_{\mathrm{curv}}(\mathfrak{K}_p(x,t))\,\mathrm{dV} = \sum_{i=1}^3\langle\partial_{\mathfrak{K}_p^i}W_{\mathrm{curv}}(\mathfrak{K}_p^1,\mathfrak{K}_p^2,\mathfrak{K}_p^3),\overline{R}_p^T\nabla(A\overline{P}.e_i)+(A\overline{R}_p)^T\nabla(\overline{P}.e_i)\rangle_{\mathbb{M}^{3\times3}}\\ &= \sum_{i=1}^3\langle\overline{R}_p\,\partial_{\mathfrak{K}_p^i}W_{\mathrm{curv}}(\mathfrak{K}_p^1,\mathfrak{K}_p^2,\mathfrak{K}_p^3),\nabla(A\overline{P}.e_i)\rangle_{\mathbb{M}^{3\times3}}+\langle\overline{R}_p\,\partial_{\mathfrak{K}_p^i}W_{\mathrm{curv}}(\mathfrak{K}_p^1,\mathfrak{K}_p^2,\mathfrak{K}_p^3)\mathfrak{K}_p^{i,T}\overline{R}_p^T,A^T\rangle_{\mathbb{M}^{3\times3}}\\ &= \sum_{i=1}^3-\langle\mathrm{Div}\left[\overline{R}_p\,\partial_{\mathfrak{K}_p^i}W_{\mathrm{curv}}(\mathfrak{K}_p^1,\mathfrak{K}_p^2,\mathfrak{K}_p^3)\right],A\overline{P}.e_i\rangle_{\mathbb{R}^3}+\langle\overline{R}_p\left(\sum_{i=1}^3\partial_{\mathfrak{K}_p^i}W_{\mathrm{curv}}(\mathfrak{K}_p^1,\mathfrak{K}_p^2,\mathfrak{K}_p^3)\mathfrak{K}_p^{i,T}\right)\overline{R}_p^T,A^T\rangle\\ &= -\langle\mathrm{Div}\left[\overline{R}_p\,D_{\mathfrak{K}_p}W_{\mathrm{curv}}(\mathfrak{K}_p)\right],A\overline{P}\rangle_{\mathbb{M}^{3\times3}}+\langle\overline{R}_p\left(\sum_{i=1}^3\partial_{\mathfrak{K}_p^i}W_{\mathrm{curv}}(\mathfrak{K}_p^1,\mathfrak{K}_p^2,\mathfrak{K}_p^3)\mathfrak{K}_p^{i,T}\,\overline{R}_p^T\right),A^T\rangle\\ &= -\langle\mathrm{Div}\left[\overline{R}_p\,D_{\mathfrak{K}_p}W_{\mathrm{curv}}(\mathfrak{K}_p)\right]\overline{P}^T,A\rangle+\langle\overline{R}_p\left(\sum_{i=1}^3\partial_{\mathfrak{K}_p^i}W_{\mathrm{curv}}(\mathfrak{K}_p^1,\mathfrak{K}_p^2,\mathfrak{K}_p^3)\mathfrak{K}_p^{i,T}\right)\overline{R}_p^T,A^T\rangle\\ &= -\langle\overline{R}_p\,\overline{R}_p^T\,\mathrm{Div}\left[\overline{R}_p\,D_{\mathfrak{K}_p}W_{\mathrm{curv}}(\mathfrak{K}_p)\right]\overline{U}_p\overline{R}_p^T,A\rangle-\langle\overline{R}_p\,\mathrm{skew}\left(\sum_{i=1}^3\left(\partial_{\mathfrak{K}_p^i}W_{\mathrm{curv}}(\mathfrak{K}_p^1,\mathfrak{K}_p^2,\mathfrak{K}_p^3)\mathfrak{K}_p^{i,T}\right)\right)\overline{R}_p^T,A\rangle\\ &= -\langle\overline{R}_p\,\mathrm{skew}\left(\overline{R}_p^T\,\mathrm{Div}\left[\overline{R}_p\,D_{\mathfrak{K}_p}W_{\mathrm{curv}}(\mathfrak{K}_p)\right]\overline{U}_p\right)\overline{R}_p^T,A\rangle-\langle\overline{R}_p\,\mathrm{skew}\left(D_{\mathfrak{K}_p}W_{\mathrm{curv}}(\mathfrak{K}_p)\mathfrak{K}_p^T\right)\overline{R}_p^T,A\rangle\,.\end{aligned}\tag{7.8}$$

Since $A\in C_0^\infty(\Omega,\mathfrak{so}(3,\mathbb{R}))$ is arbitrary, equation $(2.18)_2$ follows. In order to obtain the remaining five equations for the five independent components of $\overline{U}_p\in\mathrm{SL}(3,\mathbb{R})\cap\mathrm{PSym}(3)$ we consider the second possible independent variation of $\overline{P}$. With

$$\frac{\mathrm{d}}{\mathrm{dt}}\overline{P}=\overline{R}_p\,T\,\overline{U}_p\,,\quad T\in\mathfrak{sl}(3,\mathbb{R})\cap\mathrm{Sym}(3)\,, \tag{7.9}$$

we consider simultaneously in each space point a one parameter group of microdeformations $\frac{\mathrm{d}}{\mathrm{dt}}\hat{P}(x,t)=\overline{R}_p\,T\,\overline{U}_p$, $\hat{P}(x,0)=\overline{P}(x)$, $T\in C_0^\infty(\Omega,\mathfrak{sl}(3,\mathbb{R}))$. The corresponding stationarity condition is obtained from $\frac{\mathrm{d}}{\mathrm{dt}}_{|t=0}I(\varphi,\hat{P}(x,t))=0$. This yields again three terms: the derivatives involving $W_{\mathrm{mp}}(F,\overline{P})$ and $\Pi(\overline{P})$ are straightforward, using the definition of the one parameter group, and yield

$$\begin{aligned}\frac{\mathrm{d}}{\mathrm{dt}}_{|t=0}\Pi(\hat{P}(x,t)) &= \langle D_{\overline{P}}\Pi(\hat{P}(x,t),\frac{\mathrm{d}}{\mathrm{dt}}\hat{P}(x,t)\rangle\\ &= \langle D_{\overline{P}}\Pi(\hat{P}(x,t),\overline{R}_pT(x,t)\cdot\overline{U}_p(x,t)\rangle = \langle\overline{R}_p^T\,D_{\overline{P}}\Pi(\overline{P})\overline{U}_p,T(x,t)\rangle\\ &= \langle\mathrm{dev\,sym}\left(\overline{R}_p^T\,D_{\overline{P}}\Pi(\overline{P})\overline{U}_p\right),T(x,t)\rangle\,,\end{aligned}\tag{7.10}$$

and

$$
\begin{aligned}
\frac{\mathrm{d}}{\mathrm{dt}}_{|t=0} W_{\mathrm{mp}}(F,\hat P(x,t)) &= \langle D_{\overline U} W_{\mathrm{mp}}(\overline U,\overline U_p),\frac{\mathrm{d}}{\mathrm{dt}}\overline U\rangle + \langle D_{\overline U_p} W_{\mathrm{mp}}(\overline U,\overline U_p),\frac{\mathrm{d}}{\mathrm{dt}}\overline U_p\rangle \\
&= -\langle D_{\overline U} W_{\mathrm{mp}}(\overline U,\overline U_p),\hat P^{-1}[\frac{\mathrm{d}}{\mathrm{dt}}\hat P]\overline U\rangle + \langle D_{\overline U_p} W_{\mathrm{mp}}(\overline U,\overline U_p),T(x,t)\overline U_p\rangle \\
&= -\langle D_{\overline U} W_{\mathrm{mp}}(\overline U,\overline U_p),\hat P^{-1}\overline R_p T(x,t)\cdot\overline U_p\overline U\rangle + \langle D_{\overline U_p} W_{\mathrm{mp}}(\overline U,\overline U_p)\overline U_p^T,T(x,t)\rangle \\
&= -\langle D_{\overline U} W_{\mathrm{mp}}(\overline U,\overline U_p)\overline U^T,\overline U_p^{-1}T(x,t)\overline U_p\rangle + \langle D_{\overline U_p} W_{\mathrm{mp}}(\overline U,\overline U_p)\overline U_p^T,T(x,t)\rangle \qquad (7.11)\\
&= -\langle \overline U_p^{-1} D_{\overline U} W_{\mathrm{mp}}(\overline U,\overline U_p)\overline U^T\overline U_p,T(x,t)\rangle + \langle D_{\overline U_p} W_{\mathrm{mp}}(\overline U,\overline U_p)\overline U_p^T,T(x,t)\rangle \\
&= -\langle \operatorname{dev}\operatorname{sym}\left(\overline U_p^{-1} D_{\overline U} W_{\mathrm{mp}}(\overline U,\overline U_p)\overline U^T\overline U_p\right),T(x,t)\rangle + \langle \operatorname{dev}\operatorname{sym}\left(D_{\overline U_p} W_{\mathrm{mp}}(\overline U,\overline U_p)\overline U_p^T\right),T(x,t)\rangle\,.
\end{aligned}
$$

For the term containing the curvature part, we note

$$
\begin{aligned}
\frac{\mathrm{d}}{\mathrm{dt}}_{|t=0}\int_\Omega W_{\mathrm{curv}}(\mathfrak{K}_p(x,t))\,\mathrm{dV} &= \sum_{i=1}^3\langle\partial_{\mathfrak{K}_p^i} W_{\mathrm{curv}}(\mathfrak{K}_p^1,\mathfrak{K}_p^2,\mathfrak{K}_p^3),\overline R_p^T\nabla(\overline R_p T\overline U_p.e_i)+(\frac{\mathrm{d}}{\mathrm{dt}}\overline R_p)^T\nabla(\overline P.e_i)\rangle_{\mathbb{M}^{3\times3}} \qquad (7.12)\\
&= \sum_{i=1}^3\langle\overline R_p\,\partial_{\mathfrak{K}_p^i} W_{\mathrm{curv}}(\mathfrak{K}_p^1,\mathfrak{K}_p^2,\mathfrak{K}_p^3),\nabla(T\overline U_p.e_i)\rangle_{\mathbb{M}^{3\times3}} \\
&= -\langle\operatorname{dev}\operatorname{sym}\left(\overline R_p^T\operatorname{Div}\left[\overline R_p\,D_{\mathfrak{K}_p} W_{\mathrm{curv}}(\mathfrak{K}_p)\right]\overline U_p\right),T\rangle\,.
\end{aligned}
$$

Since $T\in C_0^\infty(\Omega,\mathfrak{sl}(3,\mathbb{R}))$ is arbitrary, equation $(2.18)_3$ follows. By splitting the possible variations of $\overline P\in\mathrm{SL}(3,\mathbb{R})$, we have implicitly used the Cartan Lie-algebra decomposition: $\mathfrak{sl}(3,\mathbb{R})=\mathfrak{so}(3,\mathbb{R})\oplus\mathfrak{p}$, $\mathfrak{p}=\{T\in\mathrm{sym}(3)\,|\,\mathrm{tr}\,[T]=0\}$.

7.5 Validation of the Finite Element implementation

Analytical solutions can be worked out for some particular boundary value problems for the linearized elastic micromorphic continuum. They can be used to check the Finite Element implementation presented in this work. An example is given here for an infinite strip in direction 1 and with $0\le x_2\le L$, L being the thickness of the strip. We look for displacement and microdeformation fields of the form:

$$
u=u_2(x_2)\,e_2,\quad p=p_{11}(x_2)\,e_1\otimes e_1+p_{22}(x_2)\,e_2\otimes e_2 \qquad (7.13)
$$

with respect to a Cartesian orhonormal basis (e_1,e_2,e_3). As a result the non vanishing components of the strain measures are

$$
\begin{aligned}
&\varepsilon_{22}=u_2',\quad \bar\varepsilon_{11}=-p_{11},\quad \bar\varepsilon_{22}=u_2'-p_{22}\,,\\
&K_{112}=p_{11}',\quad K_{222}=p_{22}'\,, \qquad (7.14)
\end{aligned}
$$

where the prime indicates differentiation with respect to the x_2 variable. The corresponding non–vanishing stress components follow from application of the linearized elasticity constitutive equations (4.27):

$$
\begin{aligned}
&\sigma_{11}=\hat\lambda u_2'+g_1(u_2'-p_{11}-p_{22})-2g_1p_{11},\quad \sigma_{22}=(\hat\lambda+2\hat\mu)u_2'+g_1(u_2'-p_{11}-p_{22})+2g_1(u_2'-p_{22})\,,\\
&\sigma_{33}=\hat\lambda u_2'+g_1(u_2'-p_{11}-p_{22})\,,\\
&s_{11}=g_1u_2'+b_1(u_2'-p_{11}-p_{22})-(b_2+b_3)p_{11},\quad s_{33}=g_1u_2'+b_1(u_2'-p_{11}-p_{22})\,,\\
&s_{22}=(g_1+2g_2)u_2'+b_1(u_2'-p_{11}-p_{22})+(b_2+b_3)(u_2'-p_{22})\,. \qquad (7.15)
\end{aligned}
$$

In the special case (4.29), the only non–vanishing components of the hyperstress tensors are

$$
S_{112}=Ap_{11}',\quad S_{222}=Ap_{22}'\,. \qquad (7.16)
$$

The stress tensors must fulfill the linearized balance equation of momentum and generalized moment of momentum (4.23) which reduce here to

$$
\sigma_{22}'+s_{22}'=0,\quad S_{112}'+s_{11}=0,\quad S_{222}'+s_{22}=0\,. \qquad (7.17)
$$

These equations lead to the following linear system of differential equations for the unknowns (u_2,p_{11},p_{22}):

$$
\begin{aligned}
0&=\bar\lambda u_2''-\bar b_1p_{11}'-\bar bp_{22}'\,,\\
0&=Ap_{11}''+\bar b_1u_2'-bp_{11}-b_1p_{22}\,,\\
0&=Ap_{22}''+\bar bu_2'-b_1p_{11}-bp_{22}\,, \qquad (7.18)
\end{aligned}
$$

where the following notations have been introduced:

$$
b=b_1+b_2+b_3,\quad \bar\lambda=\hat\lambda+2\hat\mu+2g_1+4g_2+b\,,\bar b_1=g_1+b_1,\quad \bar b=g_1+2g_2+b\,.
$$

When the displacement component u_2 is eliminated from the system (7.18), we get

$$
\begin{aligned}
0&=Ap_{11}'''-Bp_{11}'-Cp_{22}'=0\,,\\
0&=Ap_{22}'''-Dp_{11}'-Dp_{22}'=0\,, \qquad (7.19)
\end{aligned}
$$

where the following notations were introduced:

$$
B=\frac{1}{A}(b-\frac{\bar b_1^2}{\bar\lambda}),\quad C=\frac{1}{A}(b-\frac{\bar b^2}{\bar\lambda}),\quad D=\frac{1}{A}(b_1-\frac{\bar b\bar b_1}{\bar\lambda})\,. \qquad (7.20)
$$

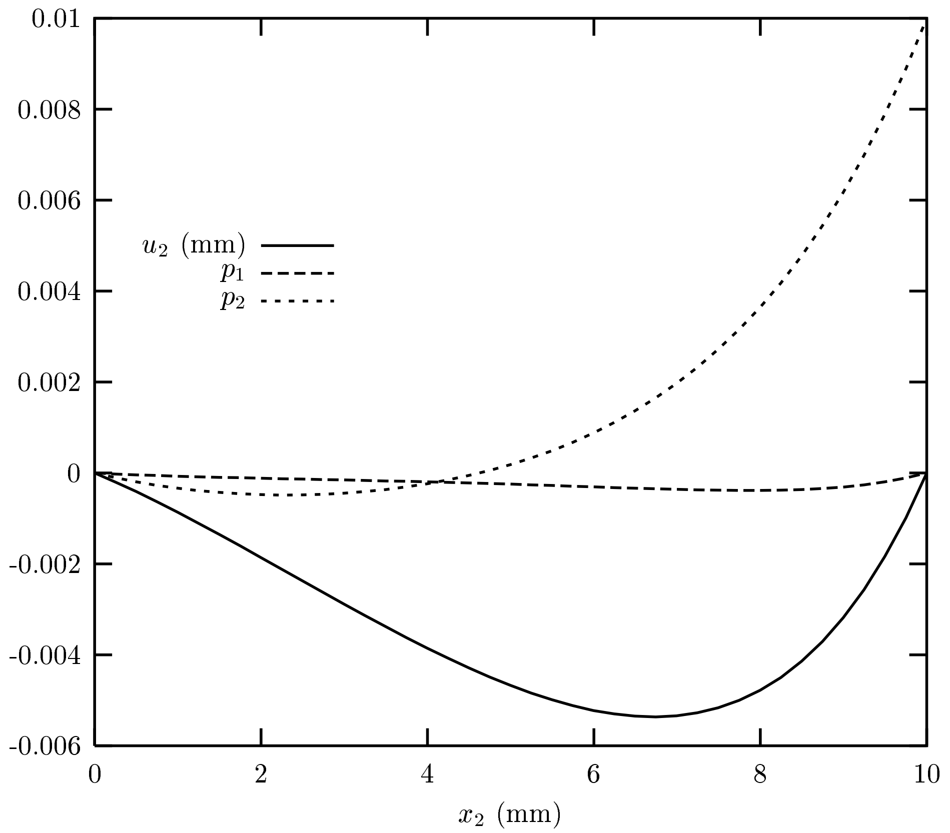

Figure 5: Displacement and microdeformation profiles along the width of an infinite strip subjected to a prescribed microdeformation $p_2 = 0.01$ at $x_2 = 10$mm. This test is used in the validation procedure of the Finite Element implementation of linear micromorphic elasticity. The used material parameters are given by (5.9).

There exists then a linear combination p of p_{11} and p_{22} such that

$$p''' = \omega^2 \, p' \, , \tag{7.21}$$

provided that

$$\omega^4 - (B + C)\,\omega^2 - C^2 = 0 \, , \tag{7.22}$$

which admits in general a single positive root. The solution of the system (7.18) is then a linear combination of $\cosh(\omega x_2)$ and $\sinh(\omega x_2)$ functions. The integration constants are determined by the proper boundary conditions. The figure 5 gives the functions $u_2(x_2), p_{11}(x_2), p_{22}(x_2)$ over the segment $[0, L]$ corresponding to the following boundary conditions:

$$u_2(0) = u_2(L) = 0, \quad p_{11}(0) = p_{11}(L) = 0, \quad p_{22}(0) = 0, \quad p_{22}(L) = p_0 \tag{7.23}$$

The set of elastic constants used for this example is given by (5.9). The particular case $L = 10$mm, $\mathrm{p}_0 = 0.01$ is illustrated in figure 5.